
Article:
Sun, Y, Harpazi, B, Wijerathna-Yapa, A et al. (2019) A ligand-independent origin of abscisic acid perception. Proceedings of the National Academy of Science, 116 (49). pp. 24892-24899. ISSN: 0027-8424

https://doi.org/10.1073/pnas.1914480116

BIOLOGICAL SCIENCES: Plant Biology

A ligand-independent origin of abscisic acid perception

Yufei Sun[1], Ben Harpazi[1], Akila Wijerathna-Yapa[1], Ebe Merilo[2], Jan de Vries[3,4], Daphna Michaeli[1], Maayan Gal[5], Andrew Cuming[6], Hannes Kollist[2], Assaf Mosquna[1*]

[1]The Robert H. Smith Institute of Plant Sciences and Genetics in Agriculture, The Hebrew University of Jerusalem, Rehovot, Israel.

[2]Plant Signal Research Group, Institute of Technology, University of Tartu, Tartu, Estonia.

[3]Institute of Microbiology, Technische Universität Braunschweig, Braunschweig, Germany.

[4]Institute of Microbiology and Genetics, Georg-August-University Göttingen, Goldschmidtstr. 1, 37077 Göttingen, Germany

[5]Department of Oral Biology, The Maurice and Gabriela Goldschleger School of Dental Medicine, Sackler Faculty of Medicine, Tel Aviv University, Tel Aviv, Isreal.

[6]Centre for Plant Sciences, Faculty of Biological Sciences, University of Leeds, Leeds, UK.

*To whom correspondence may be addressed. Email: assaf.mosquna@mail.huji.ac.il

Abstract

Land plants are considered monophyletic, descending from a single successful colonization of land by an aquatic algal ancestor. Ability to survive dehydration to the point of desiccation is a key adaptive trait enabling terrestrialization. In extant land plants, desiccation tolerance depends on the action of the hormone abscisic acid (ABA) that acts through a receptor-signal transduction pathway comprising a PYRABACTIN RESISTANCE 1-like (PYL) - PROTEIN PHOSPHATASE 2C (PP2C) - SNF1-RELATED PROTEIN KINASE 2 (SnRK2) module. Early-diverging aeroterrestrial algae mount a dehydration response that is similar to that of land plants but that does not depend on ABA: although ABA synthesis is widespread among algal species, ABA-dependent responses are not detected, and algae lack an ABA-binding PYL homologue. This raises the key question of how ABA signalling arose in the earliest land plants. Here, we systematically characterized ABA receptor-like proteins from major land plant lineages, including a protein found in the algal sister lineage of land plants. We found that the algal PYL-homologue encoded by *Zygnema circumcarinatum* has basal, ligand-independent activity of PP2C repression, suggesting this to be an ancestral function. Similarly, a liverwort receptor possesses basal activity but it is further activated by ABA. We propose that co-option of ABA to control a preexisting PP2C-SnRK2-dependent desiccation-tolerance pathway enabled transition from an “all-or-nothing” survival strategy to a hormone-modulated, competitive strategy by enabling continued growth of anatomically diversifying vascular plants in dehydrative conditions, enabling them to exploit their new environment more efficiently.

Key words

PYL, basal activity, plant evolution, *Zygnema*

Significance Statement

Synthesis of ABA and proteins required for its downstream signalling are ancient, and found in aquatic algae, but these primitive plants do not respond to ABA, and lack ABA receptors. The present work traces the evolution of ABA as an allosteric regulatory switch. We found that ancient PYLs homologs proteins have constitutive ABA-independent phosphatase-binding activity that, in land plants, has gradually evolved into ABA-activated receptor. We propose that ABA-mediated fine-tuning of the preexisting signalling cascade was a key evolutionary novelty that aided these plants in their conquest of land.

Introduction

ABA is best known for its function as a stress-related metabolite and is ubiquitous throughout the plant kingdom (1, 2). ABA is perceived by the START domain PYRABACTIN RESISTANCE 1/ PYR1-LIKE/ REGULATORY COMPONENTS OF ABA RECEPTOR (PYR/PYL/RCAR) that interacts with members of the clade A (PP2C) protein phosphatase family (3-5). PYL binding to ABA promotes formation of a receptor-ABA-PP2C ternary complex that suppresses the dephosphorylation activity of PP2Cs (6-9). This releases SNF1-RELATED PROTEIN KINASE 2s (SnRK2s) from an otherwise inhibitory complex with PP2Cs, initiating phosphorylation of transcription factors and ion channels (10, 11). The involvement of SnRK2-mediated phosphorylation in abiotic stress has been described in green algae, bryophytes and angiosperms, and modulation of SnRK2 activity by PP2Cs is highly conserved (12-15).

Based on data from *Arabidopsis*, ABA receptors have been divided into three subfamilies, I, II and III (4). Subfamilies I and II receptors are monomeric, while subfamily III receptors are dimeric and exclusive to the more recently diverged angiosperms (16). The appearance of dimeric receptors represents a dramatic evolutionary change in the perception of ABA. These subfamily III receptors require ABA for dimer dissociation, which results in low basal receptor activity in the absence of ABA (17). *In planta*, this results in a steep threshold between stress-sensitized versus relaxed physiology. Based on the evolutionary changes in the ABA perception apparatus from bryophytes to angiosperms, and on the fact that the ABA molecule preceded the emergence of ABA receptors (2, 18), we reasoned that investigating the evolution of PYL function could illuminate how ABA evolved as a hormone modulating plant stress responses during the emergence of land plants.

Results and discussion

Algal ABA biology presents a dilemma: The presence of ABA has been confirmed in many species, however, algal genomes largely do not encode PYR/L ABA receptors. Recently, the *Zygnema circumcarinatum* alga was shown to express a transcript encoding a protein apparently orthologous to PYR/Ls, designated as ZcPYL8 (19). To verify that ZcPYL8 is not an outlier of this species, we mined transcriptome resources and identified ten more transcripts with homology to PYR/Ls in four genera: *Zygnema*, *Zygnemopsis*, *Spirogyra*, *and Mesotaenium* (*SI Appendix,* Fig. S1a and S2). The sequence analysis pointed to several amino acid differences in the otherwise conserved, key ABA-binding residues

identified in *bona fide* land plant ABA receptors (*SI Appendix,* Fig. S1a). To test whether ZcPYL8 functions as an ABA receptor, we performed yeast two-hybrid and *in vitro* phosphatase inhibition assays with clade A PP2Cs. The ZcPYL8 protein interacted and inhibited both native and *Arabidopsis* PP2Cs—but in an ABA-independent manner (Fig. 1a, *SI Appendix,* Fig. S3 and S4a); notably, PP2C activity was reduced in a PYL concentration-dependent manner (Fig. 1a). This contrasted with land plant ABA receptors in which the ABA-triggered allosteric binding to PP2C and the inhibition of phosphatase activity were evident. To find out if ZcPYL8 is sufficient for enhanced ABA signaling *in planta*, we expressed the latter in the *Arabidopsis aba2-1* ABA-deficient mutant background. We reasoned that under controlled growth conditions and in the absence of ABA, stress-signaling would principally be governed by the basal receptor activity. We monitored the phenotype of the transformed lines by means of fresh weight accumulation and canopy temperature. Expression of ZcPYL8 partially rescued the mutant phenotype, exemplifying the basal activity of the algal PYL (Fig. 2a, b and *SI Appendix,* Fig. S5). Moreover, application of ABA did not result in an enhanced response compared to the response registered in *aba2-1*(Fig. 2c). On the contrary, expression of ABA responsive MpPYL1 enhanced ABA response in comparison to *aba2-1* (Fig. 2c) (20), suggesting that ZcPYL8 activates ABA signaling *in planta* in an ABA-independent fashion. An isothermal titration calorimetry assay, performed to determine whether ZcPYL8 can bind ABA, showed no thermal signature, whereas titration of liverwort MpPYL1 or *Arabidopsis* PYL10 with ABA resulted in an exothermic reaction (Fig. 2d and *SI Appendix,* Fig. S6), suggesting that ZcPYL8 is exceptionally not regulated by ABA. By mutating the obvious residues that differ between land plants and algae, we could not enhance ABA-induced ZcPYL8-PP2C interaction (*SI Appendix*, Fig. S7). However, it was evident that mutating ABA binding residues which do not take part in PP2C interaction seemingly did not hamper the receptor activity. This speaks to a pronounced flexibility in the ligand binding pocket; this flexibility has important implications for the evolution of ABA as the input signal that triggers the entire downstream cascade. Due to the lack of amino acid conservation in the specific ABA binding residues within the Zygnematophycean PYL clade (*SI Appendix*, Fig. S1b; i.e. PYR1 K59), we postulate that this ABA-independent activity presumably unique to ZcPYL8, might in fact attest a general ancestral feature of the algal PYLs. Furthermore, these results suggest that the inhibition of PP2C phosphatases is an ancestral function of PYR/L proteins that evolved as an ABA-independent process, before the origin of land plants. The question of the regulation of algal PYLs still remains open. Analysis of the published differential

transcriptomic data on *Zygnema circumcarinatum* strain SAG 2419 challenged with extreme dehydration/desiccation stress (21) showed a modest two-fold average upregulation of *ZcPYL8* transcript (*SI Appendix*, Fig. S8). As already noted by Rippin et al. (21), transcriptional regulation of core ABA signaling components is likely not the main route to initiate alga's signaling cascade (*SI Appendix*, Fig. S8). Possibly regulation can occur at protein level as suggested in Irigoyen et al. (22) or by activity modulation by different ligand.

In pursuit of traces of this ancestral ABA-independent PYL-PP2C activity in extant land plants, we analysed basal ABA-independent phosphatase inhibitory activity of PYR/L proteins across diverse land plant lineages, ranging from bryophytes to angiosperms. We tested the *Marchantia* receptor, alongside three *Physcomitrella*, five *Selaginella* and eleven *Arabidopsis* receptors. Yeast two-hybrid and phosphatase inhibition assays confirmed that land plant PYLs function as ABA receptors, as manifested by their ABA-mediated interaction with clade A PP2Cs and inhibition of PP2C activity (*SI Appendix,* Fig. S3 and S4b-e). Next, we tested the basal activity of the aforementioned PYLs using recombinant proteins for ABA-free receptor-PP2C inhibition assays (Fig. 1b-e). To further normalize PP2C activity, receptors were also tested with the *Arabidopsis* phosphatase HAB1 (*SI Appendix,* Fig. S9). For the latter, receptors were assayed in the minimal concentration needed to obtain maximal HAB1 inhibition when saturated with ABA. The *Marchantia* receptor showed 30-50% basal activity when analyzed with the native PP2C or with the standardized HAB1 (Fig. 1b and *SI Appendix,* Fig. S9). *Physcomitrella PYLs* demonstrated both ABA-induced activity and basal activity (PpPYL1, 20%; PpPYL3, 15%; Fig. 1c and *SI Appendix,* Fig. S9). Three out of the four active *Selaginella* receptors had measurable basal activity, while SmPYL2 was fully ligand-dependent (Fig. 1d and *SI Appendix,* Fig. S9). In *Arabidopsis*, the monomeric receptors included receptors exhibiting a range of basal activities, whereas subfamily III dimeric receptors had no basal activity (Fig. 1e and *SI Appendix,* Fig. S9). A decline in basal ABA receptor activity may have broadened the dynamic range of the stress response, enabling fine-tuning of the response. The predominant role of the angiosperm-exclusive dimeric receptors (with the lowest basal activity) in the collective ABA response would therefore be a manifestation of the highest level of response range, while the contrary is the case for the single *Marchantia* receptor, that seemingly provides a narrow ABA response range (50% basal activity) (Fig. 1 insertion).

While receptors displaying high basal activity might obscure ABA-mediated fine-tuning processes, *Arabidopsis*, *Striga*, *Solanum, Oryza* and *Triticum* still maintain both receptors

with a narrower response range alongside receptors that allow a broader range of response (23-27). *Arabidopsis* PYL10 stands out as an example of a receptor with high basal activity, as its regulation by ABA affects less than 50% of the response magnitude (Fig. 1e). However, we found that *PYL10* expression is undetected in available transcriptome datasets, suggesting that if it is expressed during the plant life cycle, it is either at a very low level or developmentally restricted in some way. Similarly, *Triticum* TaPYL5 showed high basal activity in phosphatase inhibition assays, signifying that it is an ABA receptor with a narrow response range, whose expression is also very restricted during the lifecycle of wheat (27). We therefore investigated the promoter specificity of *Arabidopsis PYL10*, using a 2078 bp upstream promoter sequence (*SI Appendix,* Fig. S10a) driving a *VENUS* reporter construct. We observed high expression and protein accumulation in leaves (*SI Appendix,* Fig. S10b), implying that the promoter sequence did not dictate a limited transcription pattern for *PYL10*. However, the 3' end of the *PYL10* gene, which contains sequences of two transposable elements, causes a strong transcriptional down-regulation (*SI Appendix,* Fig. S10c-e). The suppression of *PYL10* by the 3' region likely enables higher ABA-related responsiveness in *Arabidopsis*, unmasking the alternative, highly tuned receptors with a broader response range.

To find out if the basal activity of PYL10, when its expression is enabled, is sufficient to activate ABA signaling, we took advantage of the aforementioned receptor/*aba2*-1 mutant expression system. We transformed *aba2-1* with *PYL10* under the regulation of its native promoter but without its 3' region sequence. *PYL10* transcription was observed in various vegetative tissues as well as the developing seed, but not during germination (*SI Appendix,* Fig. S11). Ectopic *PYL10* expression suppressed the *aba2*-1 phenotype in both stature and thermal signature of the canopy, in agreement with its promoter-enabled expression pattern, as it did for seed maturation, size and weight (Fig. 3a-e and *SI Appendix,* Fig. S12). Furthermore, detailed analysis of whole-plant gas exchange showed that plants expressing *PYL10* had lower stomatal conductance, which was closer to wild type levels (Fig. 3c). Expression of *PYL6*, *MpPYL1* and *ZcPYL8* driven by the *PYL10* promoter resulted in similar suppression of the *aba2-1* phenotype (*SI Appendix,* Fig. S13 and 14). By contrast, the expression of *PYR1*, an entirely ABA-dependent dimeric *Arabidopsis* receptor with low basal activity, didn't suppress the aba2-1 phenotype (*SI Appendix,* Fig. S13). Thus, in the absence of external ABA, high basal receptor activity can drive what is normally the ABA response, which would otherwise have been regulated by the highly tuned dimeric receptors dominating the adaptive response in the presence of stress-triggered-ABA.

Combined with the phylogenetic relationship between PYL homologues (*SI Appendix,* Fig. S2), our results suggest that the ancestral function of PYLs was likely an ABA-independent PP2C inhibitory activity (Fig. 4). Along the evolutionary trajectory leading to the last common ancestor of land plants, PYL proteins with basal activity gained ABA-interactivity (Fig. 4). Interestingly, in case of the evolution of the auxin signaling cascade, Martin-Arevalillo and colleagues recently proposed a similar scenario that entails the modular evolution of a phytohormonal signaling cascade from a phytohormone-independent origin in streptophyte algae (28). During the evolution and diversification of land plants, the PYL protein family has expanded in a lineage-specific manner, giving rise to various character states of basal as well as ABA-dependent activity. Most recently, angiosperms gained another layer of ABA-dependency with the dimeric PYLs (Fig. 4). This suggests that a dampening of the basal activity of the receptors was a driving force for the evolution of ABA responsiveness in land plant PYLs.

In the broader sense, terrestrial stresses would have presented major challenges for the earliest land plants (29, 30). While the ability to survive desiccation would have been a necessary trait in the algal precursors of the land plants, this would be less desirable in their anatomically more complex descendants. Vegetative desiccation ceases to be a competitive evolutionary strategy when set against maintaining growth by using a hormone to initiate a range of intermediate responses. Indeed desiccation tolerance, implying the loss of all internal water, becomes a threat to survival, if the continuity of the vascular system is compromised (31). In light of the presented findings, we propose that ABA-mediated fine-tuning of the PP2C-SnRK2 signalling cascade was a key evolutionary novelty—an added layer of regulation—that aided these plants in their conquest of land (Fig. 4).

Materials and methods

Plant material

Arabidopsis thaliana aba2-1 mutant strain and its background wild type strain Columbia (Col-0) (34) were used. Unless otherwise indicated, *Arabidopsis thaliana* plants were grown in a growth chamber (Percival Scientific USA) under short-day conditions (8 h light and 16 h dark) and a controlled temperature of 20–22°C, with 70% humidity and light intensity of 70–100 μE m^{-2} sec^{-1}.

DNA sequence

Coding sequences of *ZcPYL8*, *MpPYL1*, *PpPYL1-3, SmPYL1-5, ΔN ZcABI1* (lacking N-terminal amino acids 1-247), *ΔN MpABI1* (lacking residues 1-224) and *SmABI1* were chemically synthesized (*SI Appendix,* Table 1). The *PYL10* promoter (2078 bp upstream from the PYL10 start codon) and the genomic sequences of *PYL10, PYL6* and *PYR1* were amplified from Col-0 genomic DNA. The coding sequence of *PYL10* was amplified from cDNA isolated from Col-0 seedlings. All sequences were amplified using Phusion High-Fidelity DNA Polymerase (New England Biolabs), with the exception of the *PYL10* 3' end (733 bp following the stop codon), which was amplified using KAPA HiFi HotStart DNA Polymerase (Roche).

Phylogenetic analyses of PYL sequences

To generate the dataset of PYL sequences, streptophyte algal transcriptomes were downloaded from the 1KP data (35), and a tBLASTn search was performed using all *Arabidopsis thaliana* PYLs as well as the *Zygnema circumcarinatum* ZcPYL8 as queries. For the land plants, whole-genome data of *Physcomitrella patens* (36), *Marchantia polymorpha* (20), *Selaginella moellendorffii* (37), *Azolla filiculoides* (38), *Picea abies* (39), *Triticum aestivum* (International Wheat Genome Sequencing Consortium, 2018), *Oryza sativa* (40), and *Solanum lycopersicum* (Tomato Genome Consortium, 2012) were downloaded. The 14 PYR/PYL/RCAR sequences from the *Arabidopsis thaliana* TAIR10 release were used as queries for a BLASTp search of land plant proteomes to obtain the PYL sequences. For *Oryza sativa*, and *Solanum lycopersicum*, the previously described PYL sequence annotation was used (25, 41) Incomplete and strongly truncated sequences were removed and sequences were aligned using MAFFT v7.305b (42) and the L -INS -I settings. The tree was computed using IQ-TREE multicore version 1.5.5 (Linux 64-bit built

Jun 2 2017) (43), with 1000 bootstrap replicates. This run included a determination of the best model using ModelFinder (44). ModelFinder computed log-likelihoods for 144 protein substitution models and retrieved the lowest Akaike Information Criterion, Corrected Akaike Information Criterion, and Bayesian Information Criterion for JTT+G4, which was hence solicited as the best model and used for computing the tree.

Yeast two-hybrid

The coding regions of receptors were cloned into pBD-GAL4 (Clontech) fused to the GAL4 binding domain (BD). PP2Cs were cloned into pACT (Clontech), which expresses as GAL4 activation domain (AD) protein fusion. Both pBD-GAL4 and pACT were co-transformed into *Saccharomyces cerevisiae* strain Y190, and positive colonies were selected on synthetic dextrose (SD) agar medium, lacking Leu and Trp (-LW). strains expressing receptor PP2C-combination were plated onto SD-LW containing 10 μM ABA or 0.1 % DMSO, as mock control. Following incubation at 30°C for two days, interaction was visualized by X-gal staining to monitor b-galactosidase reporter gene expression, as described previously (4).

Receptor-mediated PP2C inhibition assay

The coding sequences of *MpPYL1, PpPYL1-3, SmPYL1-5, PYL10*^{CA}, *ΔN ZcABI1* and *ΔN MpABI1* were cloned into the pET28 vector, and *ZcPYL8* was cloned into a pSUMO fusion vector, generating 6×His-tagged proteins. PYR1, PYL1-11 (except for PYL7) were described previously (45). *ΔN HAB1* (lacking N-terminal amino acids 1-178) was used to obtain 6×His-fused PP2C (46). Proteins were expressed in BL21(DE3)pLysS (Promega) *E.coli* strain. For PYLs, transformed cells were pre-cultured overnight, then transferred into 500 mL of terrific broth (TB) medium, and cultured at 30 °C to OD_{600}=0.9. IPTG (1 mM) was added, and cultures were further incubated at 15°C, overnight. For PP2C, 1 mM $MgCl_2$ and 1 mM IPTG were added at OD_{600}= 0.9, and samples were further incubated overnight, at 18°C. Cells were collected by centrifugation, suspended in buffer A (50 mM NaH_2PO_4, 300 mM NaCl, pH 8.0) plus 10 mM imidazole and stored at -80 °C. Cells were broken by two freeze-thaw cycles followed by sonication for 60s. Centrifugation was performed and cleared supernatant was loaded onto Ni-NTA agarose (Cube biotech), which was then washed with buffer A supplemented with 30 mM imidazole. Proteins were eluted with buffer A plus 250 mM imidazole. Recombinant proteins were dialyzed with 1×TBS (50 mM TRIS, 150 mM NaCl, pH 7.5), 20% glycerol, in 4°C, overnight. For purification of PP2C, 1 mM $MgCl_2$ was added to all buffers. A receptor-mediated PP2C inhibition assay was performed

as previously described (47). Reactions comprised 0.5 μM PP2C and either 0, 0.5, 1 or 2 μM receptor and 33 mM Tris·acetate (pH 7.9), 66 mM potassium acetate, 0.1% BSA, 10 mM MnCl2, 0.1% β-ME and 50 mM pNPP in the absence or presence of 10 μM ABA. Hydrolysis of pNPP was monitored at A_{405} by Epoch Microplate Spectrophotometer (BioTek). PP2C activity in the absence of receptor was set as 100% activity. The ABA dose-dependent PP2C inhibition assay was conducted as previously described (45) using 0.5 μM PP2C, and 1 μM receptor. ABA was added at 0, 0.01, 0.025, 0.05, 0.1, 1, 10 μM. PP2C activity in the presence of receptor and absence of ABA was set as 100% activity. All experiments were performed with two independent protein preparations.

Isothermal titration calorimetry

Proteins for ITC were dialyzed with ITC buffer containing 20 mM Tris pH 7.5, 150 mM NaCl, 1 mM β-mercaptoethanol. PYL10, MpPYL1, and ZcPYL8 were assayed at concentrations of 110 μM, 140 μM and 45 μM, respectively. Protein solution in the cell was titrated with the ligand (+)ABA dissolved in the dialysis buffer. The concentrations of ABA stock in the injection syringe for PYL10, MpPYL1 and ZcPYL8 were 1.1 mM, 1.4 mM and 0.45 mM, respectively, and the final diluted ligand concentration was twofold higher than that of the protein. ITC experiments were executed in ITC200 by a series of injections of 3 μL ABA into the ITC cell containing PYL, and heat was measured following the injection. The calorimetric analysis program in the Origin suite was used for data evaluation and presentation.

qRT-PCR

Arabidopsis leaf tissue was harvested and immediately frozen in liquid nitrogen. RNA was extracted using the RNeasy Plant Mini Kit (QIAGEN) followed by DNase digestion using the AMBION DNA-free™ Kit (Life Technologies) according to manufacturer's instructions. First strand cDNA from 1000ng total RNA was synthesized using SuperScript™ III Reverse Transcriptase (Thermo Fisher Scientific). qRT-PCR was performed using SYBR Green ROX Mix (Thermo Fisher Scientific) on a Rotor-Gene Q system (Qiagen). Samples were heated to 95°C for 30 sec, followed by 45 cycles of 95°C for 30 sec, 60°C for 30 sec and 72°C for 30 sec. Results were analyzed with Rotor-Gene Q Series software (Qiagen) using the ΔΔCT method.

Western blot

Total proteins were extracted from liquid nitrogen-frozen tissue followed by SDS/PAGE separation and transfer to a nitrocellulose membrane. The presence of HPB-fused protein was detected with 1:5000 streptavidin-conjugated horseradish peroxidase (GE). Images were acquired using ImageQuant LAS 4000 mini (GE) and were analyzed with ImageQuant TL 1D v8.1 software (GE).

ABA-deficient mutant phenotype suppression assay

For 35S promoter-driven *ZcPYL8* and *MpPYL1*, coding sequences of *ZcPYL8* and *MpPYL1* were cloned into pEGHPB under the control of 35S promoter. For PYL10 promoter-driven receptors, the 35S promoter was replaced by 2078-bp upstream sequence of PYL10. Then, the coding sequences of *ZcPYL8*, *MpPYL1*, *PYR1*, *PYL6* and *PYL10* were cloned into the above-mentioned vector under the control of PYL10 promoter. Constructs were stably transformed into the *Arabidopsis* ABA-deficient mutant, *aba2-1*. Sixteen independent T1 transformants for each construct were selected based on glufosinate resistance. Fresh weight and leaf temperature were monitored after two months of growth under short-day conditions. Two independent T_3 single-copy lines expressing *PYL10* were obtained for gas exchange experiments.

Thermal analysis

Two-month-old *Arabidopsis* plants grown in growth chambers at 22°C, 10 h light/14 h dark were using for thermal analysis. The thermal images of the plants were taken at 10 AM using a FLIR T630 camera (FLIR). Canopy temperature of plants was measured with Flir Tools v5.2.15161.1001 software (FLIR). Each dot in box plots represent means of 8-10 measurements of individual plant.

Gas exchange experiments

For gas exchange experiments, *Arabidopsis* seeds were planted in soil containing 2:1 (v:v) peat:vermiculite and grown well-watered in growth chambers (Snijders Scientific, Drogenbos, Belgia), under 12/12 photoperiod, 23˚/18˚C temperature, 150 µmol m^{-2} s^{-1} light and 70% relative humidity conditions, and were 25-30 days old during experiments. Whole-rosette stomatal conductances were recorded with an 8-chamber custom-built temperature-controlled gas-exchange device analogous to the one described before. Plants were inserted into the measurement cuvettes and allowed to stabilize at standard conditions:

ambient CO_2 (~400 ppm), light 150 µmol m^{-2} s^{-1} and relative air humidity (RH) ~60 ± 5%. In diurnal experiments, the dark period lasted from 8 PM to 8 AM, similar to growth chamber conditions. In ABA treatment experiments, 5 µM ABA with 0.012% Silwet L-77 (Duchefa) and 0.05% ethanol was sprayed on the leaves, and plants were put back into cuvettes and for continued measurement of leaf conductance. Photographs of plants were taken after the experiment and leaf rosette area was calculated using ImageJ 1.37v (National Institutes of Health, USA). Stomatal conductance for water vapor was calculated with a custom-written program, as previously described (48).

Site-directed mutagenesis

Mutants were generated using the QuikChange Lightning Multi Site-Directed Mutagenesis Kit (Agilent, USA) according to the manufacturer's instruction. Sequences of mutagenesis primers are provided in *SI Appendix*, Table 1.

Statistical analysis

All data were statistically analyzed using JMP pro 12 statistical package (SAS Institute). Tukey HSD test was used for fresh weight, leaf temperature, seed length and hundred-seed weight analysis. Student's *t*-test was used for qRT-PCR analysis. All box plots, bar graphs and connecting lines were generated using Origin 8.1 Software.

Data availability

Primers, sequences and accession numbers of genes analyzed in this study are listed in supplemental table. Seeds of transgenic lines used in this study are available from the corresponding authors upon request.

Acknowledgements

We thank Sean Cutler, Idan Efroni, Ori Naomi and Shahal abbo for the insightful discussions and for commenting on the ideas presented here. We thank Oded Pri-tal for graphic assistance. This research was supported by grants from the Israel Science Foundation (661/18), Israel Binational Agricultural Research and Development Fund (IS-4919-16 R) and German-Israel Foundation, Young scientists Program-(I-2410-203.13/2016) Y. S. is was supported partly by The Lady Davis Fellowship Trust for the award of a Golda Meir Fellowship. J.d.V. thanks the German Research Foundation (DFG) for a Return Grant (VR132/3-1) and the European Research Council (ERC) for funding under the European Union's Horizon 2020 research and innovation programme (grant agreement No. 852725, ERC-StG "TerreStriAL"). E.M. was supported by the Estonian Research Council (PUT1133).

Author contributions.

Y.S. conducted all the receptor and phosphatase assays, and designed and performed all the genetic analysis. B.H. and A.W.Y. helped with the generation of transgenic plants. J.d.V. performed the phylogenetic analysis and evolutionary synthesis. M.G. conducted and analyzed the ITC analysis, and E. M. and H.K. performed the stomatal conductance measurements and analysis. A.M, and Y.S designed and supervised experiments collaboratively. A.M., Y.S., D.M. and A.C.C. drafted the manuscript, with contributions from all co-authors.

References

1. E. Nambara, A. Marion-Poll, Abscisic acid biosynthesis and catabolism. *Annu. Rev. Plant Biol.* **56**, 165-185 (2005).
2. F. Hauser, R. Waadt, J. I. Schroeder, Evolution of abscisic acid synthesis and signaling mechanisms. *Curr. Biol.* **21**, R346-355 (2011).
3. Y. Ma *et al.,* Regulators of PP2C phosphatase activity function as abscisic acid sensors. *Science* **324**, 1064-1068. (2009).
4. S. Y. Park *et al.,* Abscisic acid inhibits type 2C protein phosphatases via the PYR/PYL family of START proteins. *Science* **324**, 1068-1071 (2009).
5. S. R. Cutler, P. L. Rodriguez, R. R. Finkelstein, S. R. Abrams, Abscisic acid: emergence of a core signaling network. *Annu. Rev. Plant. Biol.* **61**, 651-679 (2010).
6. K. Melcher *et al.,* A gate-latch-lock mechanism for hormone signaling by abscisic acid receptors. *Nature* **462**, 602-608 (2009).
7. K. Miyazono *et al.,* Structural basis of abscisic acid signaling. *Nature* **462**, 609-614 (2009).
8. J. Santiago *et al.,* The abscisic acid receptor PYR1 in complex with abscisic acid. *Nature* **462**, 665-668 (2009).
9. P. Yin *et al.,* Structural insights into the mechanism of abscisic acid signaling by PYL proteins. *Nat. Struct. Mol. Biol.* **16**, 1230-1236 (2009).
10. F. F. Soon *et al.,* Molecular mimicry regulates ABA signaling by SnRK2 kinases and PP2C phosphatases. *Science* **335**, 85-88 (2012).
11. T. Miyakawa, Y. Fujita, K. Yamaguchi-Shinozaki, M. Tanokura, Structure and function of abscisic acid receptors. *Trends Plant Sci.* **18**, 259-266 (2013).
12. D. Gonzalez-Ballester, S. V. Pollock, W. Pootakham, A. R. Grossman, The central role of a SNRK2 kinase in sulfur deprivation responses. *Plant Physiol.* **147**, 216-227 (2008).
13. H. Fujii, J. K. Zhu, *Arabidopsis* mutant deficient in 3 abscisic acid-activated protein kinases reveals critical roles in growth, reproduction, and stress. *Proc. Natl. Acad. Sci. USA* **106**, 8380-8385 (2009).
14. C. Lind*, et al.,* Stomatal guard cells co-opted an ancient ABA-dependent desiccation survival system to regulate stomatal closure. *Curr. Biol.* **25**, 928-935 (2015).
15. A. Shinozawa*, et al.*, SnRK2 protein kinases represent an ancient system in plants for adaptation to a terrestrial environment. *Commun. Biol.* **2**, 30 (2019).
16. T. Umezawa*, et al.*, Molecular basis of the core regulatory network in ABA responses: sensing, signaling and transport. *Plant Cell Physiol.* **51**, 1821-1839 (2010).
17. F. Dupeux*, et al.,* A thermodynamic switch modulates abscisic acid receptor sensitivity. *EMBO J.* **30**, 4171-4184 (2011).
18. W. Hartung, The evolution of abscisic acid (ABA) and ABA function in lower plants, fungi and lichen. *Funct. Plant Biol.* **37**, 806-812 (2010).
19. J. de Vries, B. A. Curtis, S. B. Gould, J. M. Archibald, Embryophyte stress signaling evolved in the algal progenitors of land plants. *Proc. Natl. Acad. Sci. USA* **115**, E3471-E3480 (2018).
20. J. L. Bowman *et al.,* Insights into land plant evolution garnered from the *Marchantia polymorpha* genome. *Cell* **171**, 287-304 e215 (2017).
21. M. Rippin, B. Becker, A. Holzinger, Enhanced desiccation tolerance in mature cultures of the streptophytic green alga *Zygnema circumcarinatum* revealed by transcriptomics. *Plant Cell Physiol.* **58**, 2067-2084 (2017).
22. M. L. Irigoyen *et al.,* Targeted degradation of abscisic acid receptors is mediated by the ubiquitin ligase substrate adaptor DDA1 in *Arabidopsis*. *Plant Cell* **26**, 712-728 (2014).
23. Q. Hao *et al.,* The molecular basis of ABA-independent inhibition of PP2Cs by a subclass of PYL proteins. *Mol. Cell* **42**, 662-672 (2011).
24. M. Gonzalez-Guzman *et al.,* Tomato PYR/PYL/RCAR abscisic acid receptors show high expression in root, differential sensitivity to the abscisic acid agonist quinabactin, and the capability to enhance plant drought resistance. *J. Exp. Bot.* **65**, 4451-4464 (2014).
25. Y. He *et al.,* Identification and characterization of ABA receptors in Oryza sativa. *PloS One* **9**, e95246 (2014).
26. H. Fujioka *et al.,* Aberrant protein phosphatase 2C leads to abscisic acid insensitivity and high transpiration in parasitic *Striga*. *Nature Plants* **5**, 258-262 (2019).
27. R. Mega *et al.,* Tuning water-use efficiency and drought tolerance in wheat using abscisic acid receptors. *Nature Plants* **5**, 153-159 (2019).
28. R. Martin-Arevalillo *et al.,* Evolution of the auxin response factors from charophyte ancestors. *PLoS Genet.* **15**, e1008400 (2019).
29. C. F. Delwiche, E. D. Cooper, The evolutionary origin of a terrestrial flora. *Curr. Biol.* **25**, R899-910 (2015).

30. A. C. Cuming, S. R. Stevenson, From pond slime to rain forest: the evolution of ABA signalling and the acquisition of dehydration tolerance. *New Phytol.* **206**, 5-7 (2015).
31. W. R. Anderegg, Spatial and temporal variation in plant hydraulic traits and their relevance for climate change impacts on vegetation. *New Phytol.* **205**, 1008-1014 (2015).
32. J. de Vries, J. M. Archibald, Plant evolution: landmarks on the path to terrestrial life. *New Phytol.* **217**, 1428-1434 (2018).
33. J. L. Morris *et al.*, The timescale of early land plant evolution. *Proc. Natl. Acad. Sci. USA* **115**, E2274-E2283 (2018).
34. K. M. Leon-Kloosterziel *et al.*, Isolation and characterization of abscisic acid-deficient *Arabidopsis* mutants at two new loci. *Plant J.* **10**, 655-661 (1996).
35. X. Wu *et al.,* Data access for the 1,000 Plants (1KP) project (2014).
36. S. A. Rensing *et al.,* The *Physcomitrella* genome reveals evolutionary insights into the conquest of land by plants. *Science* **319**, 64-69 (2008).
37. J. A. Banks *et al.,* The *Selaginella* genome identifies genetic changes associated with the evolution of vascular plants. *Science* **332**, 960-963 (2011).
38. F. W. Li *et al.*, Fern genomes elucidate land plant evolution and cyanobacterial symbioses. *Nature Plants* **4**, 460-472 (2018).
39. B. Nystedt *et al.,* The Norway spruce genome sequence and conifer genome evolution. *Nature* **497**, 579-584 (2013).
40. S. Ouyang *et al.,* The TIGR rice genome annotation resource: improvements and new features. *Nucleic Acids Res.* **35**, D883-887 (2007).
41. P. Chen *et al.,* Interactions of ABA signaling core components (SlPYLs, SlPP2Cs, and SlSnRK2s) in tomato (*Solanum lycopersicon*). *J. Plant Physiol.* **205**, 67-74 (2016).
42. K. Katoh, D. M. Standley, MAFFT multiple sequence alignment software version 7: improvements in performance and usability. *Mol. Biol. Evol.* **30**, 772-780 (2013).
43. L. T. Nguyen, H. A. Schmidt, A. von Haeseler, B. Q. Minh, IQ-TREE: a fast and effective stochastic algorithm for estimating maximum-likelihood phylogenies. *Mol. Biol. Evol.* **32**, 268-274 (2015).
44. S. Kalyaanamoorthy, B. Q. Minh, T. K. F. Wong, A. von Haeseler, L. S. Jermiin, ModelFinder: fast model selection for accurate phylogenetic estimates. *Nat. Methods* **14**, 587-589 (2017).
45. M. Okamoto *et al.,* Activation of dimeric ABA receptors elicits guard cell closure, ABA-regulated gene expression, and drought tolerance. *Proc. Natl. Acad. Sci. USA* **110**, 12132-12137 (2013).
46. A. Saez, A. Rodrigues, J. Santiago, S. Rubio, P. L. Rodriguez, HAB1-SWI3B interaction reveals a link between abscisic acid signaling and putative SWI/SNF chromatin-remodeling complexes in *Arabidopsis*. *Plant Cell* **20**, 2972-2988 (2008).
47. A. Mosquna *et al.,* Potent and selective activation of abscisic acid receptors in vivo by mutational stabilization of their agonist-bound conformation. *Proc. Natl. Acad. Sci. USA* **108**, 20838-20843 (2011).
48. T. Kollist *et al.,* A novel device detects a rapid ozone-induced transient stomatal closure in intact *Arabidopsis* and its absence in *abi2* mutant. *Physiol. Plantarum* **129**, 796-803 (2007).

Figure legends

Figure 1: Evolution of ABA receptors indicates an increase in ABA dependency as a result of reduction of basal activity.

Recombinant 6×His-Sumo-ZcPYL8 (**a**), 6×His-MpPYL1 (**b**), PpPYL1, PpPYL3 (**c**), SmPYL1-5 (**d**), PYR1, PYL1-6, PYL8, PYL10, MBP-PYL9 and -11 (**e**) were expressed in *E. coli*, purified and used in PP2C activity assays with 6×His-PP2C (ZcABI1, MpABI1, PpABI1A or HAB1). Reactions were performed with 0.5 μM 6×His-PP2C and varying concentrations of PYL (0, 0.5, 1.0, 2.0 μM) in the absence (green) or presence (orange) of 10 μM ABA. PP2C activity is expressed as percentage of activity of PP2C in the absence of receptor. Graphs plot average values from three technical repeats, and error bars indicate SD. Results shown were reproduced with three independent protein purifications. Numbers of receptors encoded by corresponding species are shown in green circles. The phylogenetic tree of plant lineages was built according to Bowman et al.(20). The length of the branches does not indicate evolutionary dating. The inserted box depicts the dynamic response range of receptor activity. The numbers on bar show the range of receptor activity from low at the left (without ABA) to high at the right (saturated with ABA). ZcPYL8 have no activity range. All the values were captured at 1:2 PP2C:PYL ratio. Plant icons are not to scale.

Figure 2. ZcPYL8 shows basal activity but no responsiveness to ABA.

ZcPYL8 or *MpPYL1* were expressed under the CaMV 35S promoter in the ABA-deficient mutant *aba2-1.* Independent T1 plants were selected based on glufosinate resistance and transplanted to soil alongside the *Col-0* and *aba2-1* controls (indicated by red and blue boxes, respectively). Suppression of ABA-deficient phenotype was scored visually based on phenotype and thermography, and quantified. **a-c** Phenotype of *aba2-1* plants expressing ZcPYL8 or MpPYL1. **a** Fresh weight, **b** and **c** Leaf temperature and thermograph. **b** before and **c**, temperature change following a day after spraying with 10 μM ABA. Photographs were captured and measurements performed after 4 weeks of growth under short-day conditions (8/16 day/night). Different letters indicate statistically significant differences (Tukey HSD test, df=3, p<0.01, for transgenic plants, n=16; for WT and *aba2-1*, n=10). **d**, Isothermal titration calorimetry (ITC) profiles and thermodynamic data from titration of ZcPYL8, MpPYL1 or PYL10 with ABA, following a series of injections of 3 μL of ABA into the ITC cell. Each peak shows the heat measured following the injection.

Figure 3: Basal activity of PYL10 is sufficient to triggers ABA physiological response. **a**, Phenotype and fresh weight of wild type (WT) (*Col-0*), *aba2-1*, and *aba2-1* mutants expressing PYL10. **b**, Thermograph and leaf temperature of WT, *aba2-1* and PYL10 transgenic plants. Photographs were taken after 6 weeks of growth under short-day conditions (8/16 day/night). Different letters indicate statistically significant differences between transgenic plants and *aba2-1* controls (Tukey HSD test, df=3, p<0.01, for transgenic plants, n=7, for WT and *aba2-1*, n=6). **c**, Diurnal changes in stomatal conductance of *Col-0*, *aba2-1*, and PYL10-expressing transgenic lines. Plants were kept in a whole-rosette gas exchange measurement device, and stomatal conductance was monitored during a diurnal light/dark cycle. **d** and **e**, Seeds of each genotypes were stratified for 4 d at 4 °C on agar medium containing 5 µM paclobutrazol (Pac) or 150 mM sodium chloride (NaCl). Germination was scored 60 h post-imbibition. Representative images were showed in **d**. Values plotted in **e** are average of three independent experiments, and error bars indicate SD.

Figure 4. Proposed scenario of the step-wise evolution of the role of PYL proteins in the PP2C-SnRK2s cascade.

The monophyletic streptophyte lineage comprises the land plants and the ZCC-grade and KCM-grade charophyte algae (green cladogram) (32). All the signal-transduction and downstream targets of ABA-signalling (PP2C, SnRK2s, transcription factors (bZIP) and ion channels (SLAC1) are present at the base of the streptophyte clade. All these algae also probably synthesize the ABA molecule (grey). Heterologous expression analysis of KCM algal (Klebsormidium nitens) components indicated existence of a regulatory “wiring” with these three components (yellow line)—suggesting its emergence already in KCM algae. Our data showed that with the gain of the PYL proteins in a common ancestor of land plants and Zygnematophyceae, the ‘basal’, ABA-independent, PP2C-inhibitory activity of PYLs was gained (orange line). The Zygnematophycean PYL homologues appear to only have basal activity, hence, designating them ‘pre-PYL’. Along the evolutionary trajectory from the algal progenitor to the last common ancestor of land plants, the basal PP2C-inhibitory activity of PYLs became supplemented by ABA-dependent activity (blue line). In angiosperms, another layer of regulation was gained with the dimeric subfamily III PYLs (purple line). All dating is based on Morris et al. (33). Species names of the streptophytes used in this study are highlighted in green.

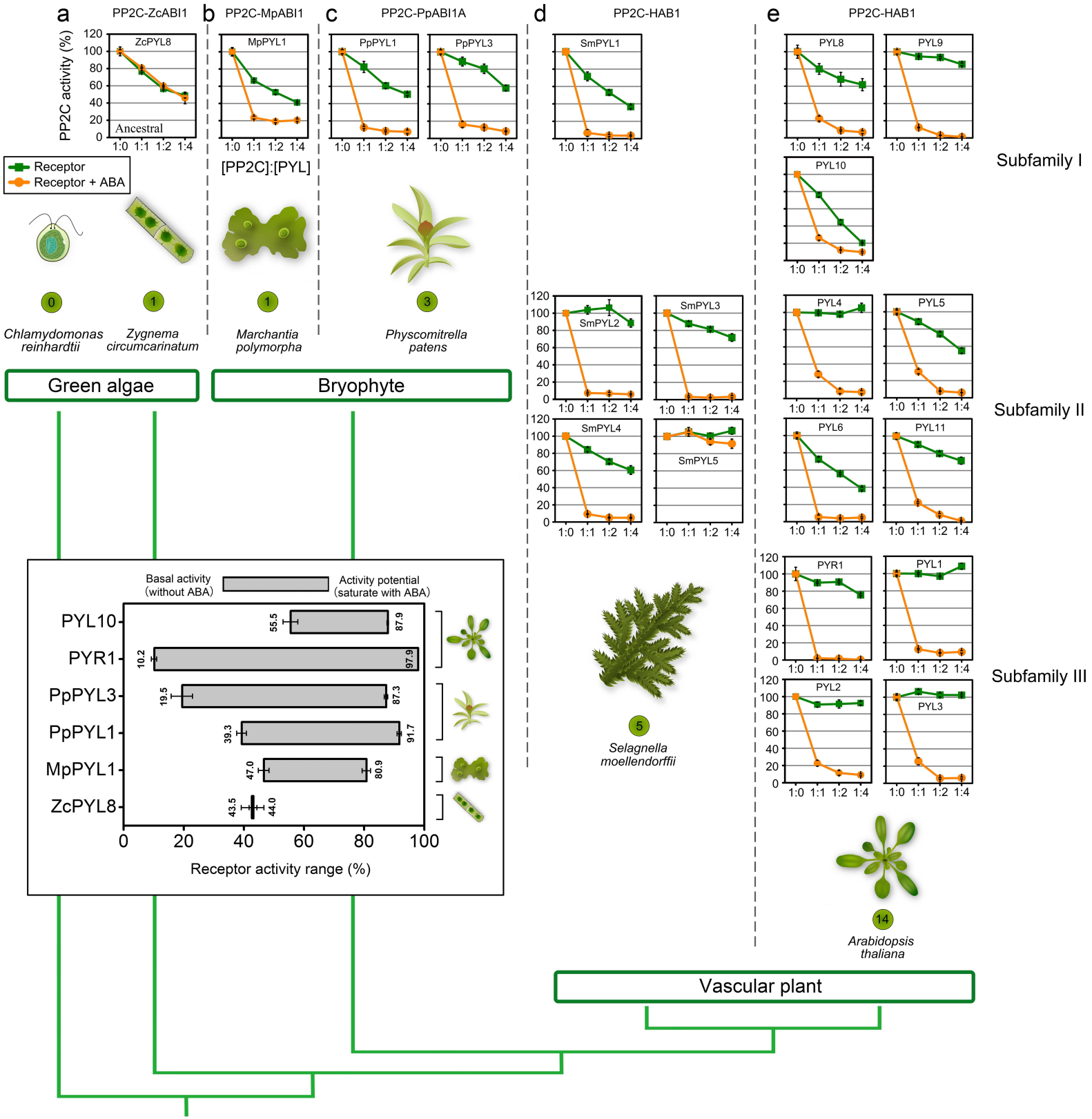
a
PP2C-ZcABI1
b
PP2C-MpABI1
c
PP2C-PpABI1A
d
PP2C-HAB1
e
PP2C-HAB1
PP2C activity (%)
ZcPYL8
Ancestral
MpPYL1
PpPYL1
PpPYL3
SmPYL1
PYL8
PYL9
PYL10
[PP2C]:[PYL]
Receptor
Receptor + ABA
SmPYL2
SmPYL3
SmPYL4
SmPYL5
PYL4
PYL5
PYL6
PYL11
PYR1
PYL1
PYL2
PYL3
Subfamily I
Subfamily II
Subfamily III
0
1
1
3
5
14
Chlamydomonas reinhardtii
Zygnema circumcarinatum
Marchantia polymorpha
Physcomitrella patens
Selagnella moellendorffii
Arabidopsis thaliana
Green algae
Bryophyte
Vascular plant
Basal activity (without ABA)
Activity potential (saturate with ABA)
PYL10
PYR1
PpPYL3
PpPYL1
MpPYL1
ZcPYL8
55.5
87.9
10.2
97.9
19.5
87.3
39.3
91.7
47.0
80.9
43.5
44.0
Receptor activity range (%)

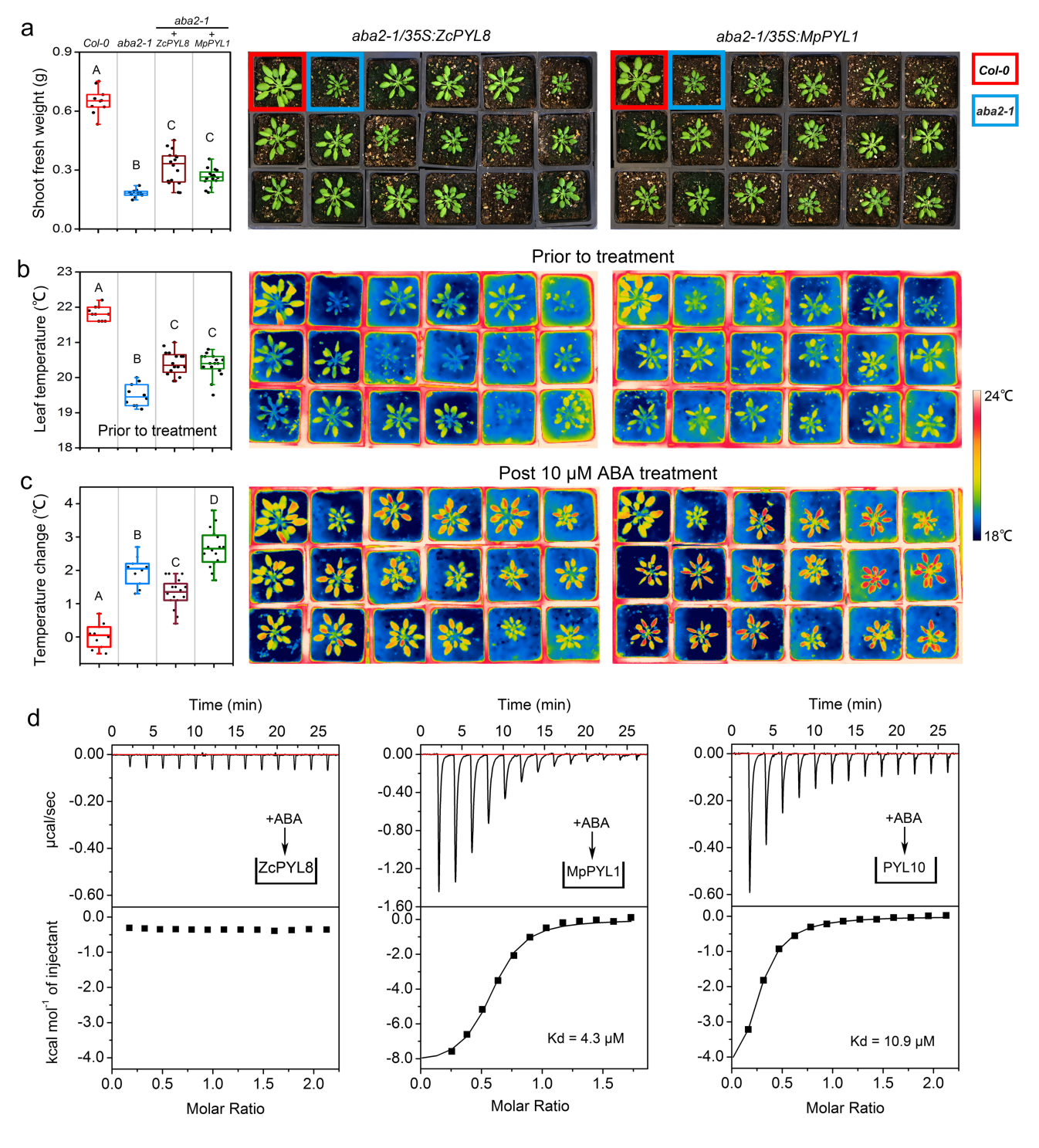
a
Col-0
aba2-1
aba2-1 + ZcPYL8
aba2-1 + MpPYL1
Shoot fresh weight (g)
A
B
C
C
aba2-1/35S:ZcPYL8
aba2-1/35S:MpPYL1
Col-0
aba2-1
b
Leaf temperature (℃)
Prior to treatment
24℃
18℃
c
Temperature change (℃)
Post 10 μM ABA treatment
D
d
Time (min)
μcal/sec
kcal mol-1 of injectant
+ABA
ZcPYL8
MpPYL1
PYL10
Kd = 4.3 μM
Kd = 10.9 μM
Molar Ratio

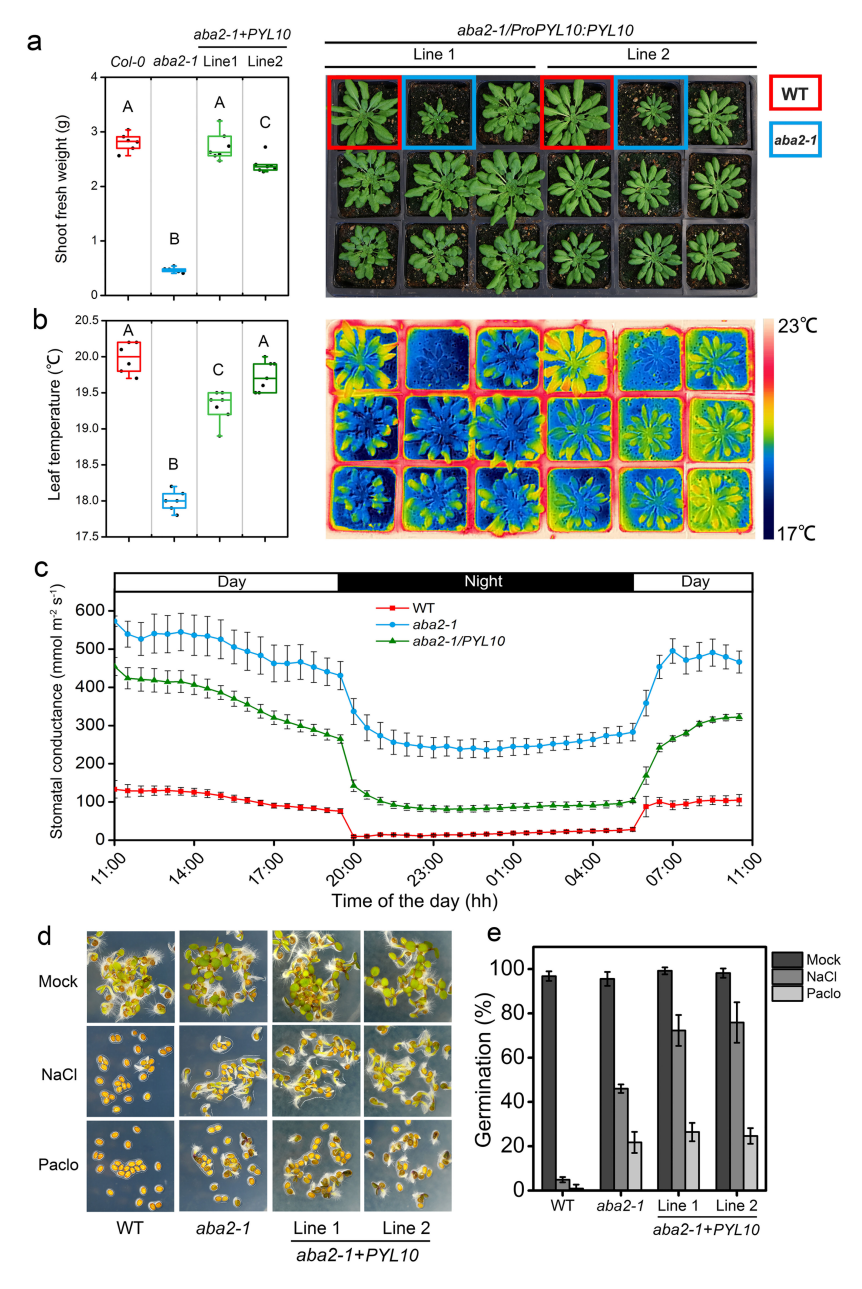
a
aba2-1+PYL10
Col-0
aba2-1
Line1
Line2
Shoot fresh weight (g)
A
B
A
C
aba2-1/ProPYL10:PYL10
Line 1
Line 2
WT
aba2-1
b
Leaf temperature (℃)
A
B
C
A
23℃
17℃
c
Day
Night
Day
WT
aba2-1
aba2-1/PYL10
Stomatal conductance (mmol m-2 s-1)
11:00
14:00
17:00
20:00
23:00
01:00
04:00
07:00
11:00
Time of the day (hh)
d
Mock
NaCl
Paclo
WT
aba2-1
Line 1
Line 2
aba2-1+PYL10
e
Germination (%)
Mock
NaCl
Paclo
WT
aba2-1
Line 1
Line 2
aba2-1+PYL10

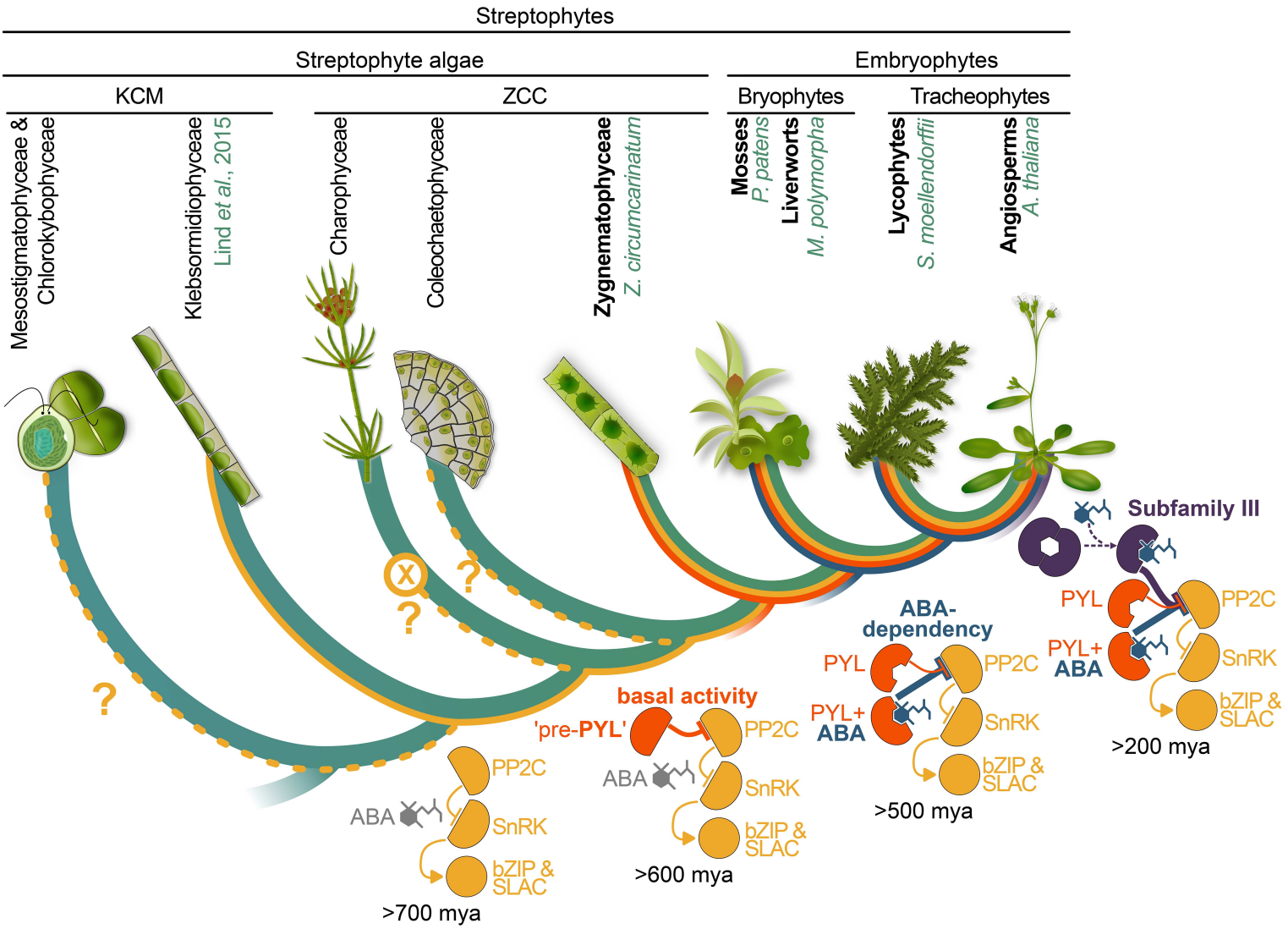
Streptophytes
Streptophyte algae
Embryophytes
KCM
ZCC
Bryophytes
Tracheophytes
Mesostigmatophyceae & Chlorokybophyceae
Klebsormidiophyceae Lind et al., 2015
Charophyceae
Coleochaetophyceae
Zygnematophyceae Z. circumcarinatum
Mosses P. patens
Liverworts M. polymorpha
Lycophytes S. moellendorffii
Angiosperms A. thaliana
?
X
?
?
PP2C
ABA
SnRK
bZIP & SLAC
>700 mya
basal activity
'pre-PYL'
PP2C
ABA
SnRK
bZIP & SLAC
>600 mya
ABA-dependency
PYL
PP2C
PYL+ ABA
SnRK
bZIP & SLAC
>500 mya
Subfamily III
PYL
PP2C
PYL+ ABA
SnRK
bZIP & SLAC
>200 mya

a

Species	Accession	Similarity to ZcPYL8 (%)	Similarity to PYR1 (%)
Zygnema sp	WGMD_scaffold_3006375	90	31
Zygnemopsis sp	MFZO_scaffold_2023374	53	32
Mesotaenium kramstae	NBYP_scaffold_2052735	50	37
Mesotaenium endlicherianum	WDCW_scaffold_2003929	34	31
Mesotaenium endlicherianum	WDCW_scaffold_2003930	22	21
Mesotaenium endlicherianum	WDCW_scaffold_2003931	31	26
Mesotaenium endlicherianum	WDCW_scaffold_2004115	31	28
Mesotaenium endlicherianum	WDCW_scaffold_2004116	33	33
Mesotaenium endlicherianum	WDCW_scaffold_2008285	33	40
Spirogyra pratensis	GBSM01001793	16	22

b

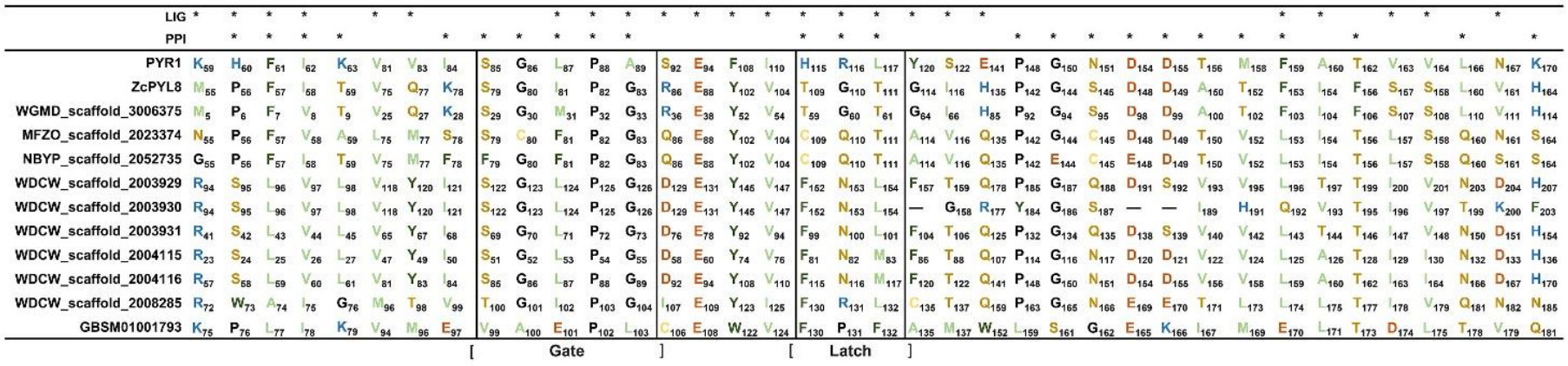

SI Appendix, Fig. S1 Putative ancestral PYR/L proteins from Zygnematophyceae species.

a, Putative PYR/L proteins from various Zygnematophyceae species. **b**, Alignment of 38 residues involved in ABA and type 2C phosphatase (PP2C) binding to orthologous ABA receptors. The gate and latch loop positions are labeled at the bottom. Asterisks indicate residues that interact with ABA [LIG] or PP2C [PPI], according to the structure of PYL2-ABA and PYL2-HAB1 (6). Amino acid sequences are color-coded according to similarities of side-chain characteristics.

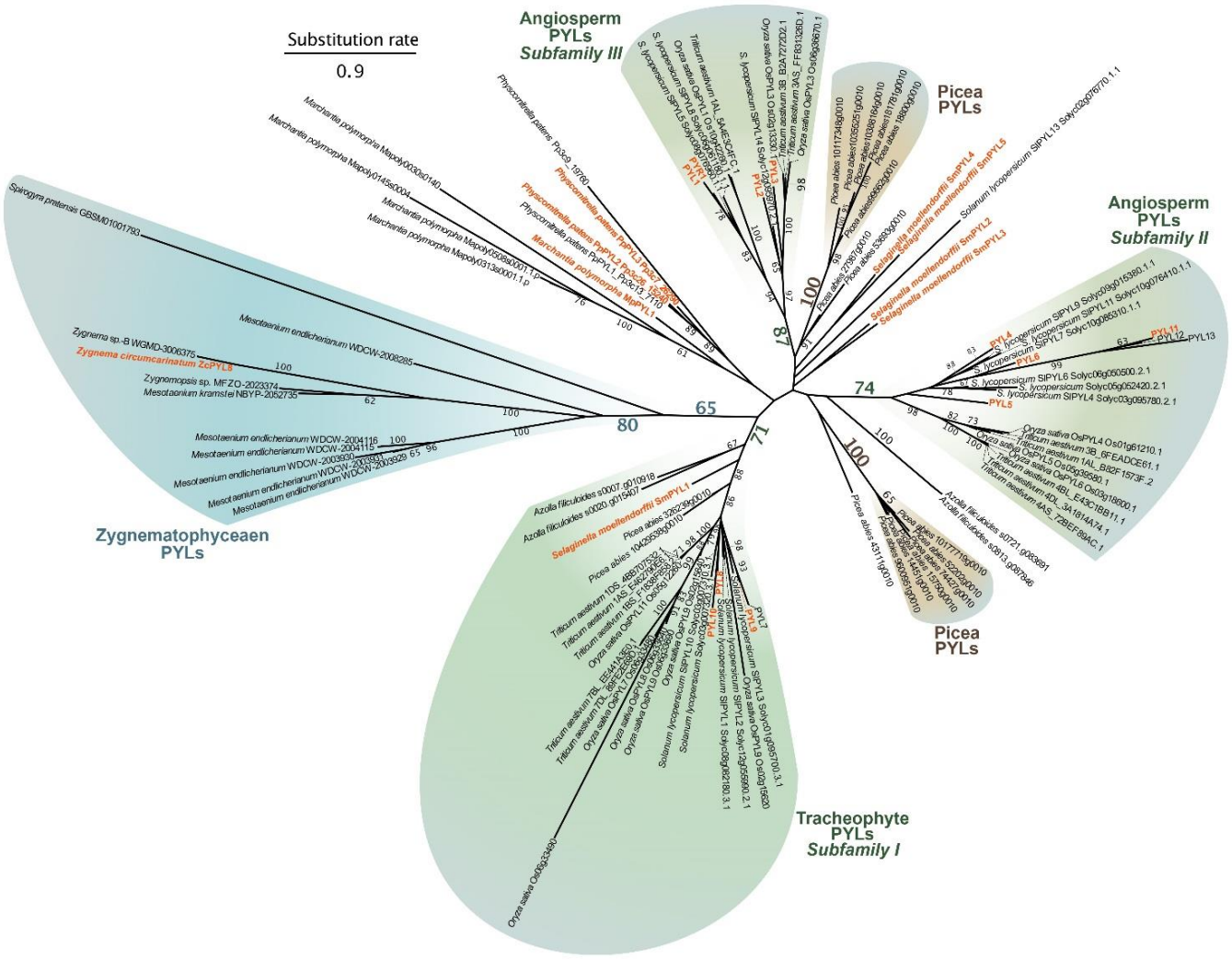

SI Appendix, Fig. S2: Unrooted phylogeny of PYL proteins across representative streptophytes.

Maximum likelihood phylogeny of 101 PYL protein sequences from representative land plant genome and streptophyte algal transcriptome data. The tree was computed based on a MAFFT L -INS -I alignment (101 sequences with 1159 columns and 562 patterns, 276 informative sites, 743 constant sites) using the JTT+G4 model, which was chosen according to ModelFinder, and 1000 bootstrap replicates (values ≥60 [%] are shown). All meaningful and well-supported clades are labeled; note the clade of Zygnematophycean and tracheophyte PYLs. Subfamilies I, II, and III were denoted based on previous studies (3). Further note that the multiple PYL accessions of *Mesotaenium endlicherianum* probably represent isoforms.

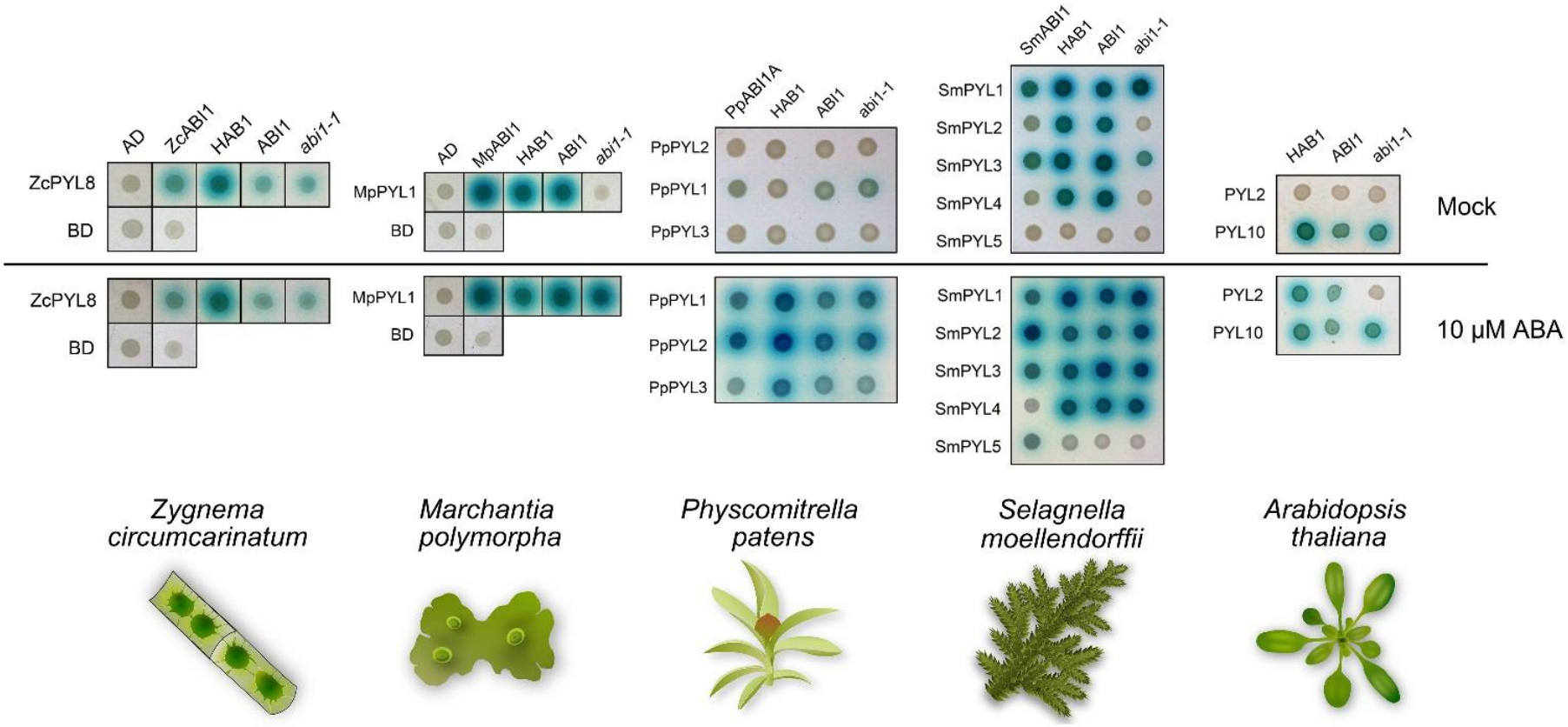

SI Appendix, Fig. S3. ABA receptors from different plant lineages interact with group A PP2Cs in yeast.

PYL-like proteins from *Zygnema circumcarinatum* (Zc), *Marchantia polymorpha* (Mp), *Physcomitrella patens* (Pp), *Selaginella moellendorffii* (Sm) and *Arabidopsis thaliana* were constructed as binding-domain fusions and tested in a yeast two-hybrid assay for interaction with activation domain-fused *A. thaliana* HAB1, ABI1, ABI1^{G180D} (encoded by the *abi1-1* allele) and endogenous group A PP2C in the presence of Mock (0.1% DMSO) (top) and 10 µM ABA (bottom).

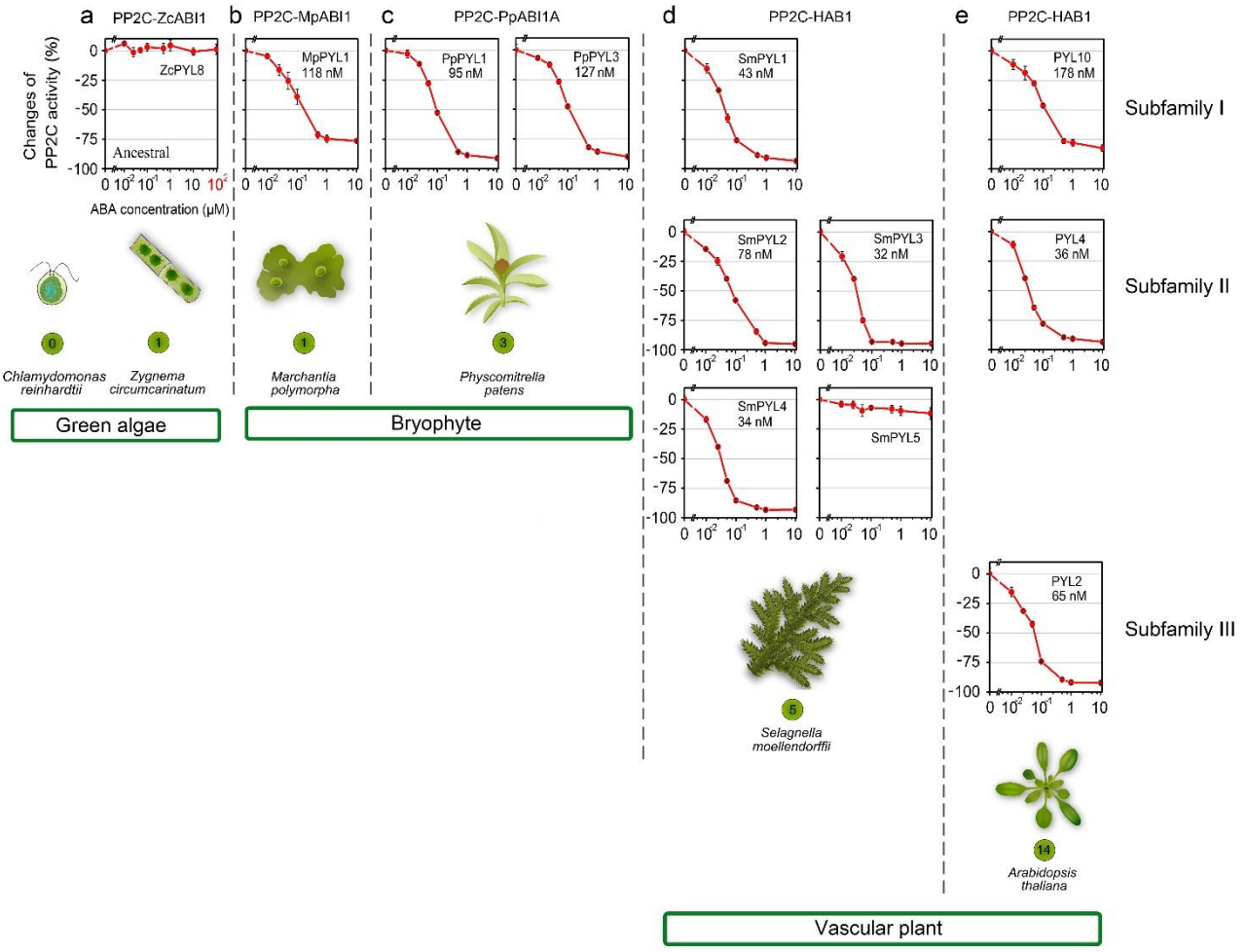

SI Appendix, Fig. S4. Land plant PP2C activity is inhibited by PYR/L receptors in an ABA dose-dependent manner.

a, Recombinant 6×His-ZcABI1 activity was measured in the presence of 6×His-SUMO-ZcPYL8 and ABA. **b**, 6×His-MpABI1 activity was measured in the presence of 6×His-MpPYL1 and ABA. **c**, 6×His-PpABI1A activity was measured in the presence of 6×His-PpPYL1 and PpPYL3. **d** and **e**, 6×His-HAB1 activity was measured in the presence of 6×His-SmPYL1-5 (**d**), PYL2, PYL4, PYL10 (**e**) and ABA. The reaction contained 0.5 μM 6×His-PP2C and 1.5 μM recombinant receptor with increasing concentrations of ABA (0, 0.01, 0.025, 0.05, 0.1, 1, 10 μM, for ZcPYL8 up to 100 μM). Phosphatase activity was calculated with three technical replicates and error bars indicate SD. Numeric values represent the ABA concentration required to activate ABA receptors to a PP2C inhibition level of 50%. The number of receptors encoded by corresponding species is shown in green circles.

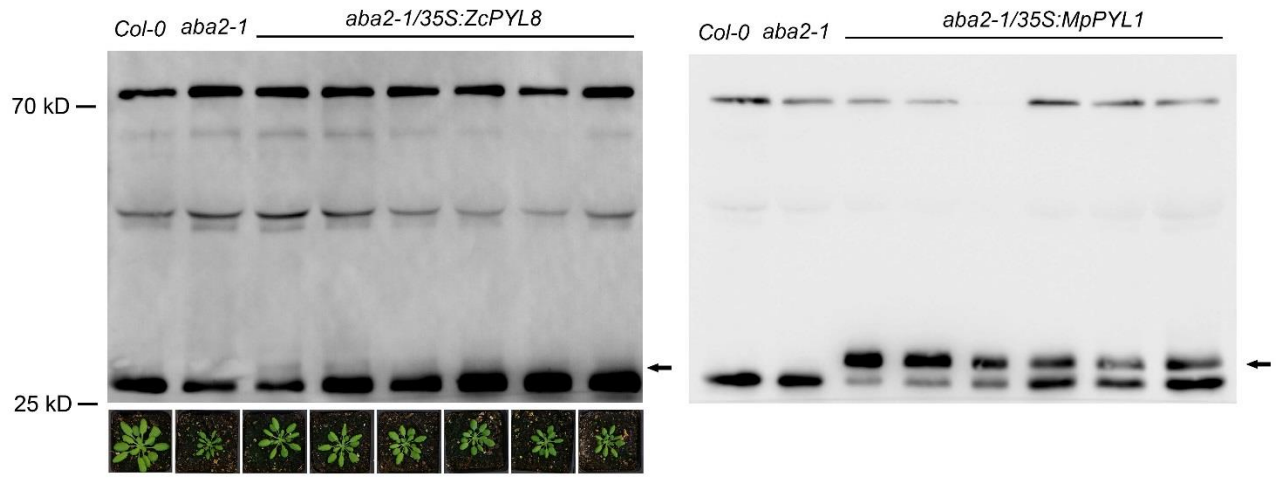

SI Appendix, Fig. S5. Verification of 35S-driven ZcPYL8 and MpPYL1 protein expression by western blot.

Total protein extracts from four-week-old leaves were separated on 15% (ZcPYL8) or 18% (MpPYL1) SDS/PAGE. Proteins were detected by HRP-conjugated streptavidin and recombinant PYL proteins were indicated by black arrow. Phenotypes of the corresponding plants are shown below, indicating that ZcPYL8 protein level correlated with plant phenotype.

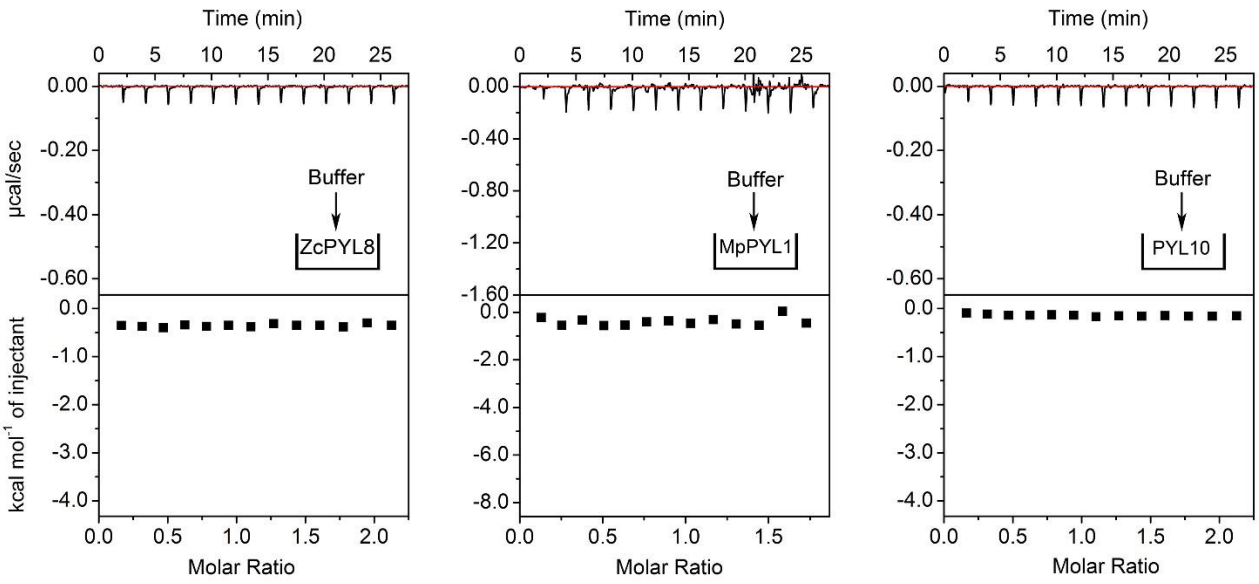

SI Appendix, Fig. S6. Control isothermal titration calorimetry assay for figure 2. Injections of TIC buffer into 45 µM ZcPYL8 (right), 140 µM MpPYL1 (middle) and 110 µM PYL10 (left), respectively.

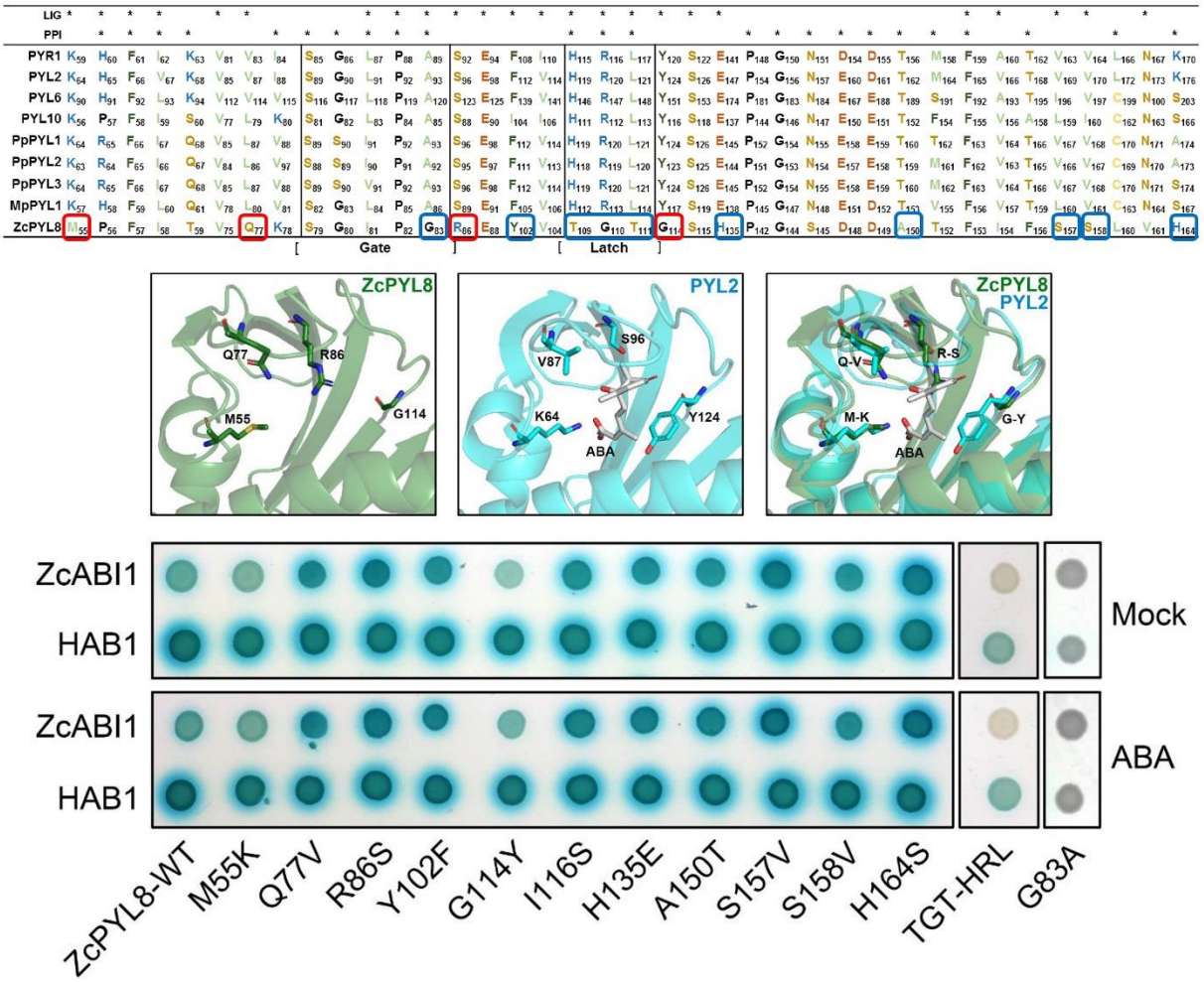

SI Appendix, Fig. S7. Mutation of the residues that differ between land plants and algae could not enhance ABA-induced ZcPYL8-PP2C interaction.

a, Alignment of residues involved in ABA and PP2C binding of orthologous ABA receptors. Boxes indicated the ligand-binding residues that differ between land plants and algae. **b**, Structural comparison of ZcPYL8 and ABA-bound PYL2 (Protein Data Bank ID 3Kb0) indicated differ key amino acids (indicated by red box in **a**) in ligand binding pocket. ZcPYL8 protein structure was computed by I-TASSER. **c**, Interactions of mutant ZcPYL8 with ZcABI1 or HAB1 were tested via yeast two-hybrid assay in the presence of Mock (0.1% DMSO) and 10 μM ABA.

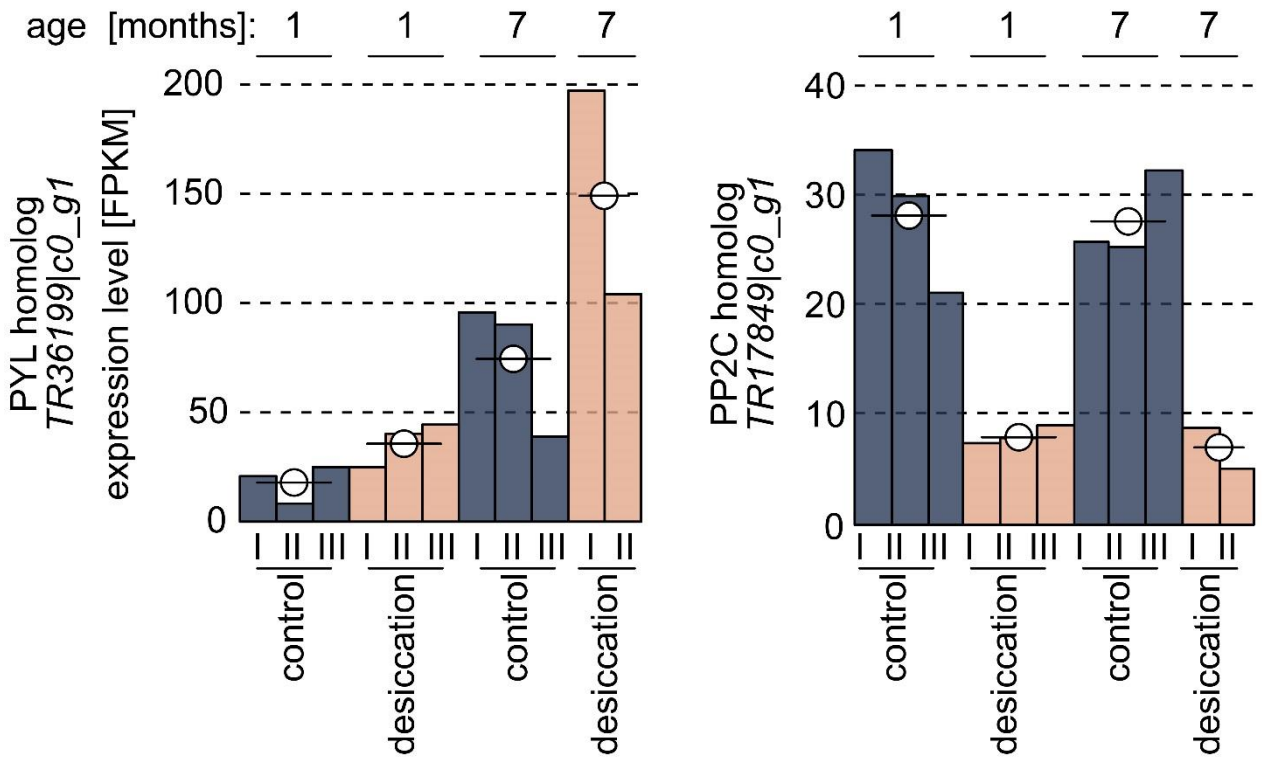

SI Appendix, Fig. S8. Expression levels of core ABA signaling components in desiccation-stressed *Zygnema circumcarinatum* SAG 2419.

Differential RNAseq data from Rippin et al. (21) on 1-month and 7-month old desiccation-stressed Zygnema circumcarinatum SAG 2419 was obtained; a BLASTx/tBLASTn search was performed to identify homology to proteins encoded by the well-annotated genome of Arabidopsis thaliana (Araport11 protein release 2016). Gene expression levels in Fragments Per Kilobase of transcript, per Million mapped reads (FPKM) of transcripts homologous to A.thaliana ABA core signaling components were plotted. On the left, a bar graph of the expression profile of the PYL homolog of Zygnema circumcarinatum SAG 2419, TR36199|c0_g1, is shown. TR36199|c0_g1 is 97.8% identical on the amino acid sequence level to ZcPYL8, which is encoded in the transcriptome of Z. circumcarinatum strain SAG698-1a used by de Vries et al. (19). On the right, a bar graph of the expression profile of a PP2C ("ZcABI1") homolog of Zygnema circumcarinatum SAG 2419, TR17849|c0_g1, is shown. TR17849|c0_g1 is 96.8% identical on the amino acid sequence level to ZcABI1, which is encoded in the transcriptome of Z. circumcarinatum strain SAG698-1a used by de Vries et al. (19).

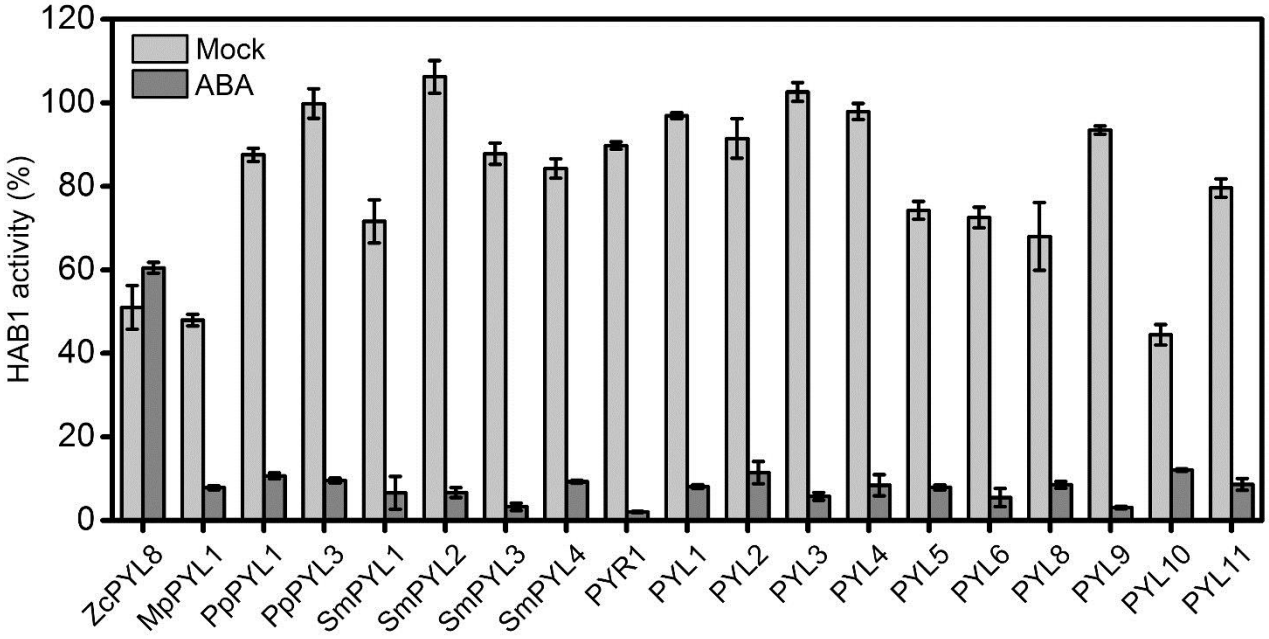

SI Appendix, Fig. S9. HAB1 activity inhibition by receptor, with or without ABA.

Recombinant receptors were assayed with HAB1 at the minimal concentration that achieved maximal HAB1 inhibition when saturated with 10 μM ABA. The HAB1 activities in the same receptor/HAB1 ratio without ABA reflect receptor basal activity. PP2C activity is expressed as percentage of PP2C activity in the absence of receptor. Graphs plot average values are from three technical replicates, and error bars indicate SD.

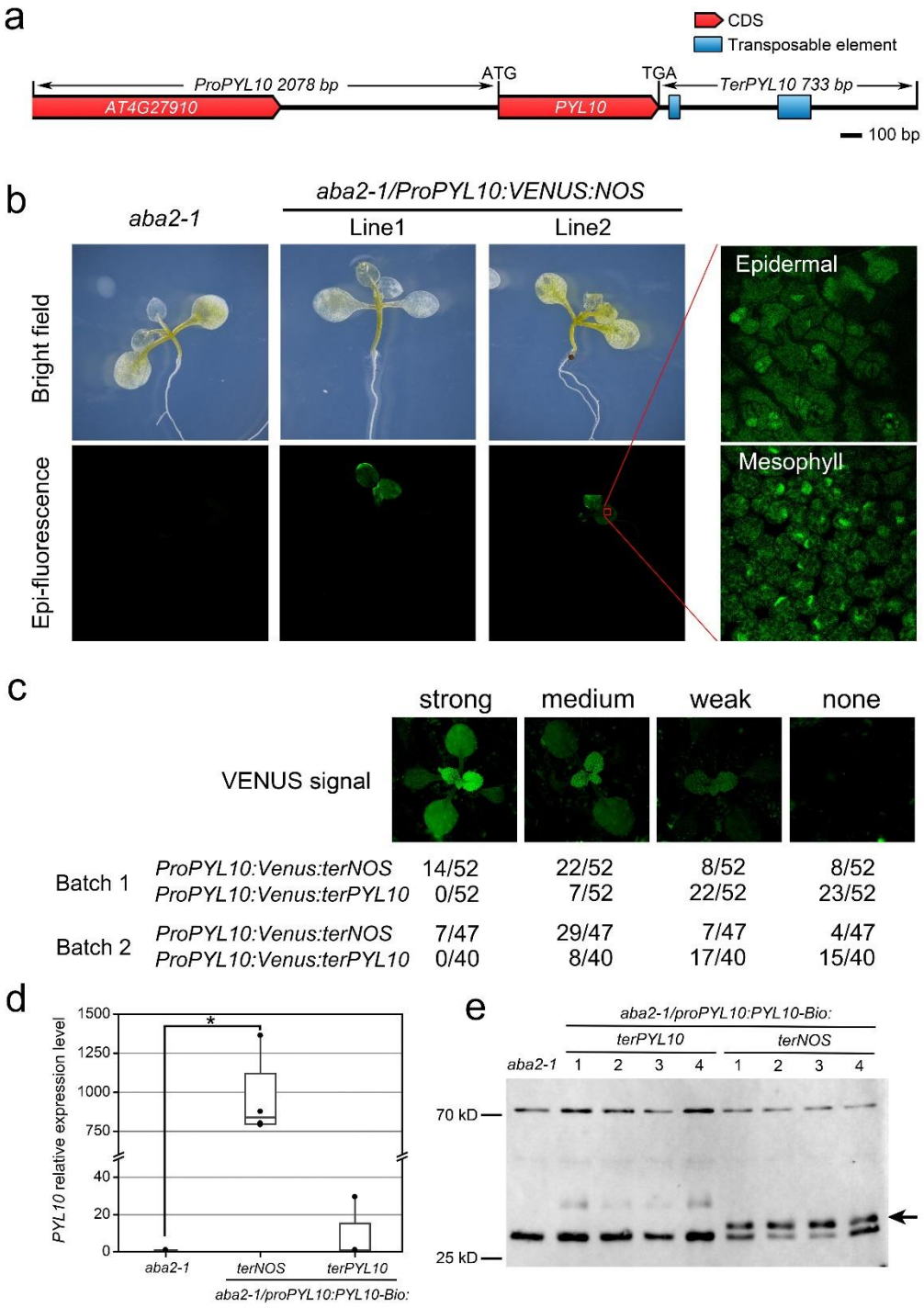

SI Appendix, Fig. S10: *PYL10* is transcriptionally suppressed by its 3' sequence.

a, Illustration of *PYL10* gene. 2078 bp upstream of the start codon was used as the *PYL10* promoter. 733 bp downstream of the stop codon was used as the *PYL10* terminator. Red boxes indicate coding sequences, blue boxes indicate predicted transposable elements. **b**, The *PYL10* promoter is active in leaves. Epifluorescence and bright-field images of seedlings of the *aba2-1* background *and ProPYL10:VENUS:NOS* transgenic lines. GFP fluorescence are observed in true leaves of *ProPYL10:VENUS:NOS* plants. **c**, Termination by the 3' end of

PYL10 results in low expression. The *Arabidopsis aba2-1* mutant was transformed with *VENUS* driven by the *PYL10* promoter and the *NOS* or *PYL10* terminators. Approximately 100 independent T1 transgenic plants, from two independent seed batches for each construct, were selected based on glufosinate resistance. GFP fluorescence was tested two weeks after germination. Signal strength was classified into four categories (see c top panel). The numerator of each value is the number of plants that showed corresponding GFP expression and the denominator is the total number of plants tested. **d** and **e**, Expression of *PYL10* is suppressed by *PYL10* termination and prevents PYL10 protein accumulation. HPB-tagged genomic sequences of *PYL10* were expressed in *aba2-1* background under the control of endogenous promoter and *NOS* or *PYL10* terminators. Independent T1 transgenic plants for each construct were selected as described above. Transcript abundance of *PYL10* was measured by qRT-PCR (**d**) and PYL10 protein was detected by western blot (**e**). Each sample represents a mixture of 10 independent two-week-old T1 seedlings. For qRT-PCR, *PEX4* was used as an internal reference. Asterisk indicates significant difference (Student's t test, $p < 0.01$). For western blot, protein was detected by HRP-conjugated streptavidin. Black arrow indicates expected recombinant PYL10 protein.

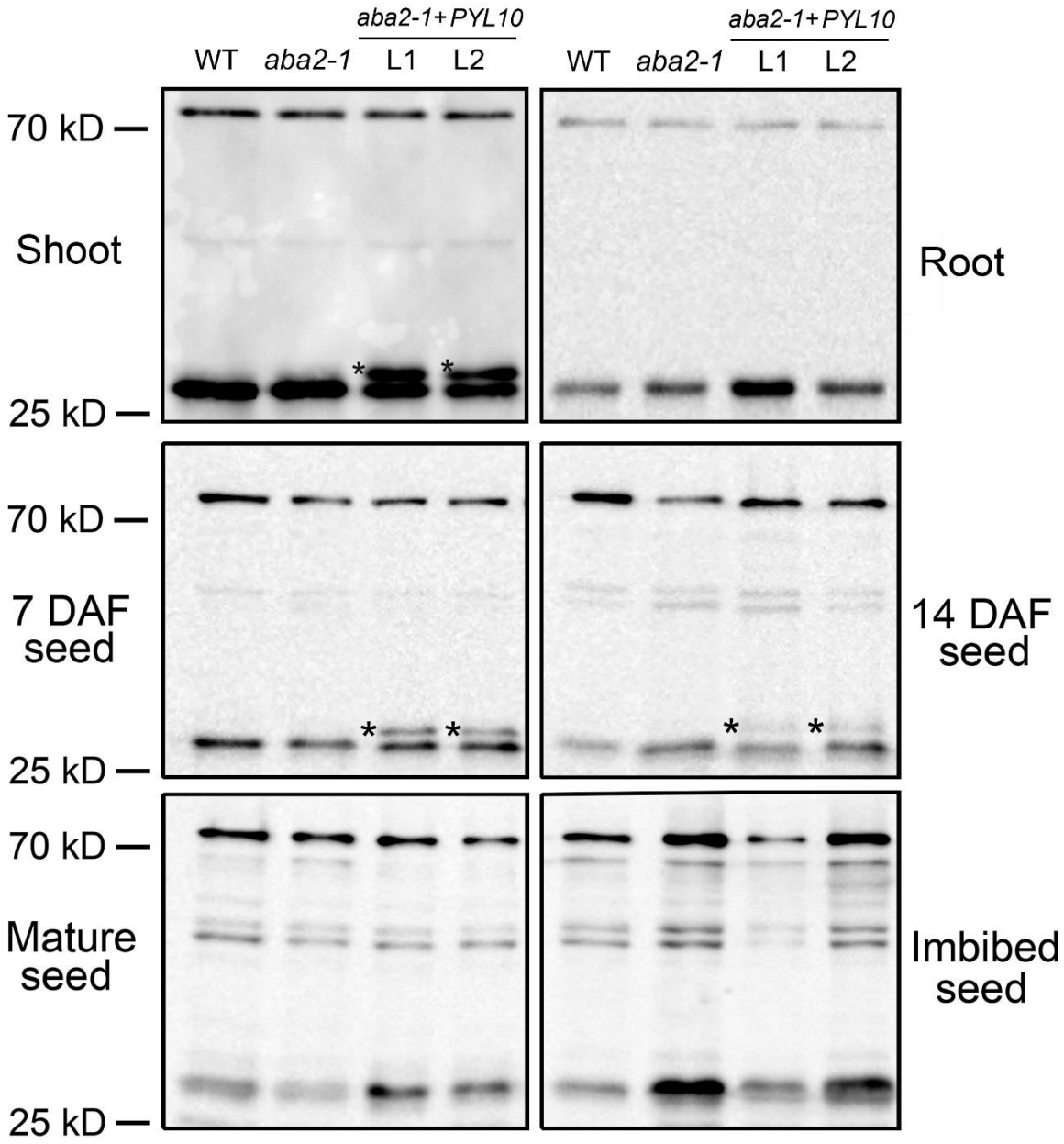

SI Appendix, Fig. S11. Expression of PYL10 and in different tissue.

Protein accumulation of *PYL10* promoter-driven HPB-tagged PYL10 in *aba2-1* background (*aba2-1+PYL10*) was verified by western blot. Total protein extracts from 10-day-old seedling shoot, roots, seeds 7 or 14 days after flowering (DFA), mature seed and 1-day imbibed seed of each genotype were separated on 15% SDS/PAGE, and then transferred to a nitrocellulose membrane. Protein was detected by HRP-conjugated streptavidin. Expected retention of recombinant protein is labeled with an asterisk.

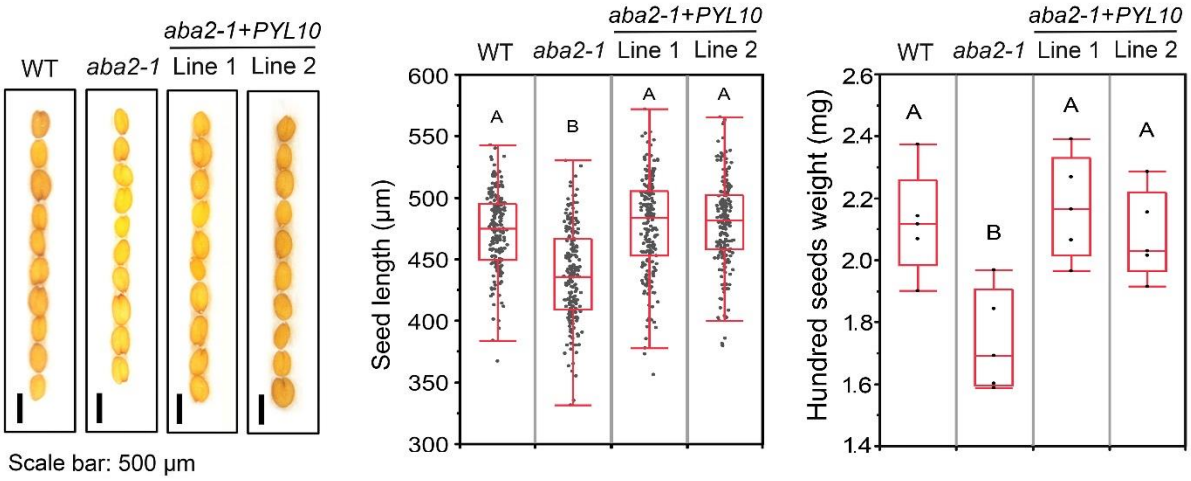

SI Appendix, Fig. S12. PYL10 suppresses ABA deficiency phenotype in seed.

Mature seeds from each genotype were collected and seed length and hundred-seed weight were measured. (Left) Representative images of mature seeds. (Middle) Seed length of each genotype, n=200. (Right) Hundred-seed weight of each genotype, n=5. Data with significant difference (Tukey HSD test, df=3, $p < 0.05$) are indicated by different letters.

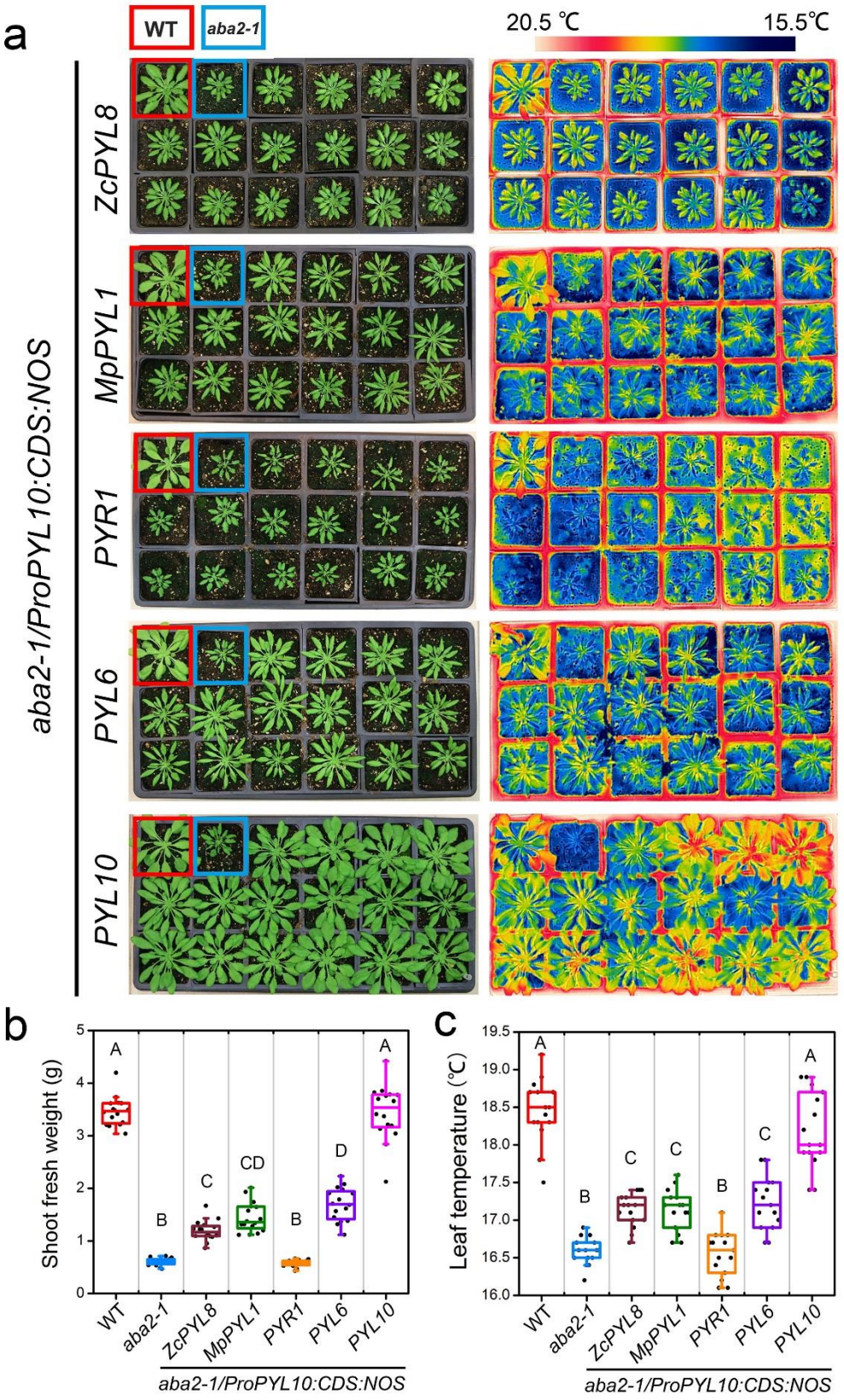

SI Appendix, Fig. S13. Receptor with basal activity drives ABA responses *in planta* in the absence of ABA.

Expression of receptors with high basal activity (ZcPYL8, MpPYL1, PYL6 and PYL10) and

low basal receptor gene (PYR1) in the *aba2-1* background. Independent T1 plants were selected based on glufosinate resistance and transplanted to soil alongside with *Col-0* and *aba2-1* (first and second pot of each tray respectively). Suppression of ABA-deficient phenotype was scored visually based on phenotype and thermography (**a**) and quantified (**b** and **c**). Photographs and measurement were performed after 6 weeks of growth under short-day conditions (8/16 day/night). Different letters indicate statistically significant differences (Tukey HSD test, df=6, n=16, p<0.01).

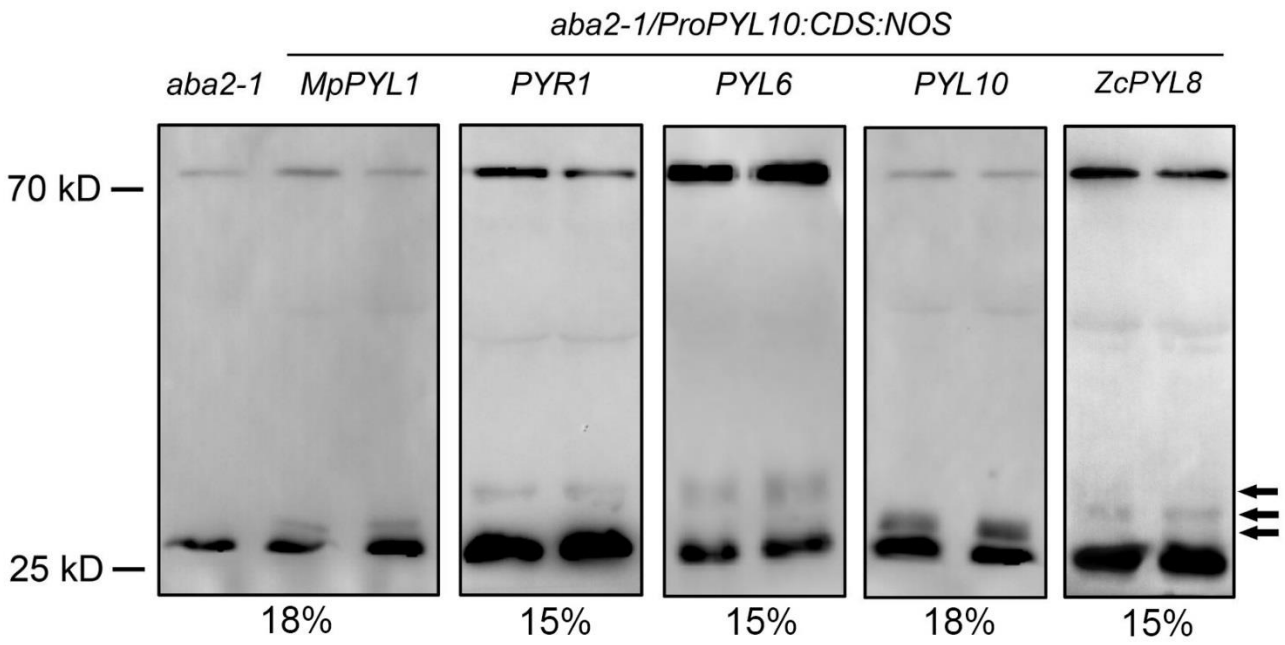

SI Appendix, Fig. S14. Verification of PYL10 promotor-driven PYL protein expression by western blot.

Expression of PYL10-driven HPB-tagged PYL protein was verified by western blot. Total protein extracts from six-week-old leaves were separated on different concentrations of SDS/PAGE (indicated below). Proteins were detected by HRP-conjugated streptavidin. Expected migration of recombinant proteins is indicated by black arrows.

SI Appendix, Table 1 List of primers used in the work. 1

Name	Sequence
pET-PYL10-F	CTGGTGCCGCGCGGCAGCCATATGAACGGTGACGAAACAAAGA
pET-PYL10-R	CGAGTGCGGCCGCAAGCTTGTCATATCTTCTTCTCCATAGATTCTG
pSUMO-ZcPYL8-F	CCGCGAACAGATTGGAGGTGGAATGGCTGTGGCAGTTATTTCT
pSUMO-ZcPYL8-R	AGTGGTGGTGGTGGTGGTGCTTAGGGAGATAACTTGAAATTTTGA
pET-PpABI1A-F	AATCTTTATTTTCAGGGCGCCATGAGTGTGCCGTGTTTTG
pET-PpABI1A-R	GTCGACGGAGCTCGAATTCGCTATCTACTACTGGGAAATTTCAGA
pACT-ZcABI1-F	ATGGCCATGGAGGCCCCGGGGATGGTCGCAACTAACAGGGC
pACT-ZcABI1-R	ATCTACGATTCATAGATCTCTTACCAATTCGTTTTTACCGATTC
pACT-MpABI1-F	ATGGCCATGGAGGCCCCGGGGATGATTCCCAGCAGCAGCG
pACT-MpABI1-R	ATCTACGATTCATAGATCTCCTACGCCGAAGATCCCGTC
pACT-PpABI1A-F	ATGGCCATGGAGGCCCCGGGGATGAGTGTGCCGTGTTTTGC
pACT-PpABI1A-R	ATCTACGATTCATAGATCTCCTATCTACTACTGGGAAATTTCAGATCC
pACT-SmABI1-F	ATGGCCATGGAGGCCCCGGGGATGGCCGTATCAGGTACCG
pACT-SmABI1-R	ATCTACGATTCATAGATCTCTTAGCGGCGCATACTAGAACT
pBD-ZcPYL8-F	AAAAAAGAATTCATGGCTGTGGCAGTTATTTCTTC
pBD-ZcPYL8-R	AAAAAAGTCGACTTAGGGAGATAACTTGAAATTTTGA
pBD-MpPYL1-F	AAAAAAGAATTCATGCTGGCGGGCGCAGAG
pBD-MpPYL1-R	AAAAAAGTCGACCTATACTTCACTCTTAATCTTCAG
pBD-PpPYL1-F	AAAAAAGAATTCATGCAGACGAAAGGACGTCAA
pBD-PpPYL1-R	AAAAAAGTCGACCTACACTTGCACAGCCTCCTTC
pBD-PpPYL2-F	AAAAAAGAATTCATGCAGGAGAAACAGGGGC
pBD-PpPYL2-R	AAAAAAGTCGACCTACGGTGCCGCTGGTTTC
pBD-PpPYL3-F	AAAAAAGAATTCATGCAGCAAGTAAAGGGGCG
pBD-PpPYL3-R	AAAAAAGTCGACTCAGGTGCAAATTACAGTACTGGA
pBD-SmPYL1-F	AAAAAAGAATTCATGAGCAGCAACGCATTGTCT
pBD-SmPYL1-R	AAAAAAGTCGACTCACGGACTCCTGGAGGCC
pBD-SmPYL2-F	AAAAAAGAATTCATGTACCAACTTACTGACGAAGAGG
pBD-SmPYL2-R	AAAAAAGTCGACTCATCTGGCCTGGTGAAGCT
pBD-SmPYL3-F	AAAAAAGAATTCATGGAAGAGGCAGTGGGTGA
pBD-SmPYL3-R	AAAAAAGTCGACCTAAACCGCGTGGGGCAAA
pBD-SmPYL4-F	AAAAAAGAATTCATGCTGGTCTCTTTAGGCGCT
pBD-SmPYL4-R	AAAAAAGTCGACTCACCGATCCTGATGCTGTTG
pBD-SmPYL5-F	AAAAAAGAATTCATGTTAACGCCCCAACAGCG
pBD-SmPYL5-R	AAAAAAGTCGACTCACTCTGGTTGCTGCTGCTG
ProPYL10-F (Overlap with pGEHPB)	AGTCAGGCCTTAATTAAGAGCTATTCCTCACCACACAAGGGG
ProPYL10-R	CGTTATCTTAAATAGCAGCAAT
Venus-F (Overlap with ProPYL10)	TGCTGCTATTTAAGATAACGATGGTGAGCAAGGGCGAG
Venus-R1 (Overlap with TerNOS)	GGAAATTCGCCTCGACCTAGGATCCTCACGAGGCCCTTTCGTCC
Venus-R2 (Overlap with TerPYL10)	AAGTCACATCTCACGAGGCCCTTTCGTC
TerPYL10-F1 (Overlap with Venus)	CTCGTGACTAGGTCGAGGAGGATGTGACTTGAGAATCTTTTCATTCG
TerPYL10-F2 (Overlap with HPB)	AGGGTAAGTCGAGAAGCTTGGATGTGACTTGAGAATCTTTTCATTCG
TerPYL10-R (Overlap with pGEHPB)	CTAGCTTATCGAATTAATTCCTTGGGTTTACCTTAAACTAAACCGT
PYL10-qRT-F	GAGCGAGTACATCAAGAAACACC
PYL10-qRT-R	CCTCACAATTGACCACACCT
PEX4-qRT-F	CAGTCCTCTTAACTGCGACTCA
PEX4-qRT-R	GGCGAGGCGTGTATACATTT
PYL10-F (Overlap with ProPYL10)	TGCTGCTATTTAAGATAACGATGAACGGTGACGAAACAAAGAAG
PYL10-R (Overlap with HPB)	TAAGGGTACTCGAGCCCGGGGAATATCTTCTTCTCCATAGATTC
ZcPYL8-F1 (Overlap with ProPYL10)	TGCTGCTATTTAAGATAACGATGGCTGTGGCAGTTATT

ZcPYL8-F2 (Overlap with p35S)	ACACGGGGACTCTAGCGCTACCATGGCTGTGGCAGTTATT
ZcPYL8-R (Overlap with HPB)	CAGGAACGTCATAAGGGTACTCGGGAGATAACTTGAAATTTTGA
MpPYL1-F (Overlap with ProPYL10)	TGCTGCTATTTAAGATAACGATGCTGGCGGGCGCAGAG
MpPYL1-F (Overlap with p35S)	ACACGGGGACTCTAGCGCTACCATGCTGGCGGGCGCAGAG
MpPYL1-R (Overlap with HPB)	TAAGGGTACTCGAGCCCGGGGAATACTTCACTCTTAATCTTCAGGTTG
PYR1-F (Overlap with ProPYL10)	TGCTGCTATTTAAGATAACGATGCCTTCGGAGTTAACACCAG
PYR1-R (Overlap with HPB)	TAAGGGTACTCGAGCCCGGGGAACGTCACCTGAGAACCACTTC
PYL6-F (Overlap with ProPYL10)	TGCTGCTATTTAAGATAACGATGCCAACGTCGATACAGTTTC
PYL6-R (Overlap with HPB)	TAAGGGTACTCGAGCCCGGGGAACGAGAATTTAGAAGTGTTCTCGGC
ZcPYL8 M55K	GATTTCAGAAATCCACATGTATGGAAGCCATTTATCACAAGCT
ZcPYL8 Q77V	GAGCCCATCGTCTGGTTCTTGTAAAGTCCGGTATTCCCGGA
ZcPYL8 G83A	GTCCGGTATTCCCGCATCATGGAGGAGAG
ZcPYL8 R86S	TCCGGTATTCCCGGATCATGGAGCAGAGAGCGATTGGACCTCCTT
ZcPYL8 Y102F	ACCAAGAGAAAGTGATGGTGTTCACTGTTGTGGATGGCGATACTG
ZcPYL8 I116S	CTGGCACAAAGAATGGATCATCCACAGTATGTGTACGGGAGGCA
ZcPYL8 G114Y	GCGATACTGGCACAAAGAATTATTCAATTACAGTATGTGTACGGGA
ZcPYL8 H135E	GGCTAATCAGCCTTGTGCAGGAGTGTTACCTCTTACCTCCACCC
ZcPYL8 A150T	CTGGAAGCACCAAAGACGATACCCTCACATTCATTTCTTTCTCCTCTC
ZcPYL8 S157V	CCCTCACATTCATTTCTTTCGTCTCTCGCCTGGTCCTCCGA
ZcPYL8 S158V	TCACATTCATTTCTTTCTCCGTTCGCCTGGTCCTCCGACATC
ZcPYL8 H164S	CCTCTCGCCTGGTCCTCCGAAGCCTCGCCACATATGCGGAGAG
ZcPYL8 TGT-HRL	GATGGTGTACACTGTTGTGGATGGCGATCATCGCTTAAAGAATGGATCAAT TACAGTATGTGTAC

1
2

SI Appendix, Table 2. List of sequences synthesized in this work. 1

Name	Sequence
ZcPYL8	ATGGCTGTGGCAGTTATTTCTTCTCCTGCAAGCTTTGCAGTGATGCCTCAAGTCAAGTCAGTAGA GAGGGAGGTGGTATGCAGTATTCTGGAAGAGAGGATCCATGCTCCTGTCGATGCTGTTTGGAG TATCCTGCGTGATTTCAGAAATCCACATGTATGGATGCCATTTATCACAAGCTGTGAGATGACTG GAGAAGTGGAAAGGGGAGCCCATCGTCTGGTTCTTCAAAAGTCCGGTATTCCCGGATCATGGA GGAGAGAGCGATTGGACCTCCTTGATGACCAAGAGAAAGTGATGGTGTACACTGTTGTGGATG GCGATACTGGCACAAAGAATGGATCAATTACAGTATGTGTACGGGAGGCAGTATATGAAGGAA GGCTAATCAGCCTTGTGCAGCACTGTTACCTCTTACCTCCACCCCCTGGAAGCACCAAAGACGA TGCCCTCACATTCATTTCTTTCTCCTCTCGCCTGGTCCTCCGACATCTCGCCACATATGCGGAGAG TCTGGCTCTGGAGATGGCAGTCAATCAAAATTTCAAGTTATCTCCCTAA
ZcABI1(Del 1-247)	ATGGTCGCAACTAACAGGGCGAGAGCTCCAATAGTAAGTATATGTAATAGTGGAAGAATAGATG GGACTTTTGCTTTTGACGACTGTCCTTCACATGGGACTCTCTCTCTTTGTGGTCGCCGCCGTGAA ATGGAGGATGCTGTCGCAATTATTCCGTCTTTTGCGGTGGTTCCATGTGGAAGTGCCGTTGGTT GTCAAGCAGCTGGAGGAGAAATAGGTGACTGTCAGATGCACTTTTTTGCAGTTTACGATGGTC ACGGTGGCTGTCAGGCTGCGAATTACTGTGCAGAGAGACTCCACAATGTTTTAGCTCACGAGC TAAAACAATCGTTGGCAAAAGCTTCACCGTTGCACGAAAAAATGCATGAAAAAACACTTATGGA GAATCATTGGCGTACGGCTATGAGGAATTCTTTTTTACGAATGGATGCTGAGATTAGTGGCCATT GTTATGGAAGCTCCGGTTCTTCTTGTCAGAGACAAAATAGTTGTCCTCACGAACCCCTCGCTCCA GAAACGGTTGGTTCTACTTCAGTTGTGGCAGTTGTGGGAGTTTCTCAAATTATTGTGGGAAATG CGGGTGATTCACGAGCTGTTTTGTCAAGAGGAGGAAAGGCTATTCCTCTCTCTATTGATCATAA GCCGGAACGCGAGGATGAAATGAAGAGAGTGGAACAGGCAGGAGGACGAGTTATATTCTGG AATGGATATCGGGTTCTTGGAGTTTTAGCCATGTCAAGGGCTATCGGCGACAGATATTTAAAACC TTATGTTATTCCTGAGCCTGAGGTGACATTTACGGAAAGAACGGGAGAGGACGAGTGCATTATT TTGGCAAGTGATGGGCTGTGGGATGTTATATCAAATGATGTCGCATGTGAAATTGCTCGTCGATG TTTATCTAAACAATACGGAGGAAGCATAGGACGAGTGGGATCCGGCAATTCGACTTTATCGACT GCAGAGGTAGAGGAAGTCGAGGGACCCGGGGCGGCTATTGCTGCGACAGTACTGACGAAACT TGCTCTAGCGCGCGGTAGTGGAGACAATATAAGTGTCGTCGTGGTCGATCTCAAAGCAAAGCAC GCGAAATCATTGCCATTGGAAAAAAACGAATCGGTAAAAACGAATTGGTAA
MpPYL1 (Optimized)	CTGGTGCCGCGCGGCAGCCATATGCTGGCGGGCGCAGAGAGAGACTTGGTTGAAAGAGACCT GGTGGAAAGACACCATAATCAGGAGATTCTTGAACATCAGTGCGGTTCTACCTTATACCAGGAG ATAGATGCGCCAGTAGAGTTGGTCTGGTCGATAGTAAGACGTTTCGACCAGCCTCAGTCCTATA AGCACTTCTTGCAGTCTAGTTCCCTGCTGATTGGAGAAGGAGCACCGGGTTCCGTGCGTGAAG TGAGACTTGTTTCTGGACTGCCAGCTACCAACAGTATCGAGCGTCTTGAGGTGCTTGATGACGC TAACCACGTGTCATCATTCCGCGTTCTTGGAGGAGGTCACCGTCTGAAGAATTATTGGAGCGTT ACCAGTCTGCATGAGCGTGTCTCCAATGGGAGACGCAAAACCATGGTAATAGAATCTTATGTAG TGGACGTACCTGAAGGTAATTCCAAAGAAGACACTATGGTCTTTGTTGATACTCTTGTACGCTGT AACCTTAAGTCACTGACCACGGTGGCAGAACAAACAGTCCTTCAGACTACTACGAGCAACCTG AAGATTAAGAGTGAAGTATAGCAAGCTTGCGGCCGCACTCG
MpABI1(Del 1-244bp)	ATGATTCCCAGCAGCAGCGGTAGTGTGAACGTTATTGACGATGGTCACTGTCCTCCTCATGGGC TTGTATCTGTTTGTGGCCGACGTCGAGAGATGGAGGATGCAGTTGCCGCTGTTCCTGCGTTTTT ATCAGTGCCATGCGATGTCACTGGTTGTAATTGCCGAGAGAATTATGGAGTTCATGCCCCTTTAC ACTTCTTTGGAGTATATGATGGACATGGAGGCTCTCAGGCAGCTGTGTTTTGTGCAGATCGTCTC CATCATGCCCTTGCAGAGGAAATGAAGACTGTTTTGAACTCTGGAAACAGTAGGATGGGATGC TCTCAGGGTAACTGGGATCTTCAATGGCGGAAGGCCATGTCAGCCTGCTTCCTCCGGATGGATG CGGAGGTTGGAGGTGTCCCTTGGAAAGTTGGACAAGCTGATAGTGAAGCTGGAAGTTCCAAG TGCTCAACAGATGCAATCGCTCCAGAGACAGTGGGCTCGACTGCTGTTGTGGCTGTAGTTGGTT CTTCTCAGATTATCGTCGCGAATTGCGGAGATTCACGGGCTGTTCTCTCACGTGGTGGGAGAGC AATTGCACTTTCAAAAGATCACAAGCCTGAACGCGAAGACGAGATGGCTAGAGTGGAGGCTG CGGGCGGTCGGGTTATCTTTTGGAACGGTTACCGTGTTTTGGGTGTACTCGCTATGTCGAGGGC CATCGGTGATAGATATCTCAAGCCCTTCGTGATCGCGGAGCCAGAGGTCACTTGCACCGTGCGA TCGGAAGATGATGAATGTTTGATCTTGGCTAGTGATGGTTTGTGGGATGTTTTATCGAACGAACT GGTTTGCGAAATAGCGCGCAAGTGCTTGATTGGTCGTCGAAATAGTGATCTTGCATTGAGTGTG

	CGTTCTGGGTTGGACGAAGAAACAGGGGAGTCCCCTGCCTCTGTGGCGGCTGCACTTCTTACC AAGCTCGCCCTAGCACGAGGCAGTAGTGACAACATTAGTGTAGTAGTTGTTGACTTAACGACGG GATCTTCGGCGTAG
PpPYL1	ATGCAGACGAAAGGACGTCAAGCTGATTTCCAGACCCTGCTAGAGGGACAGCAGGATCTGATA TGCCGGTTCCACAGACATGAACTCCAGCCACACCAGTGCGGCTCCATCCTCTTGCAGCTGATCA AGGCGCCTGTGGAGACTGTGTGGTCGGTGGCTAGAAGCTTTGACAAGCCGCAAGTATACAAGC GCTTTATCCAGACTTGTGAAATTATTGAAGGCGATGGCGGGGTGGGTAGCATCCGTGAGGTGC GCTTAGTGTCTAGTATTCCGGCAACATCGAGTATTGAGAGGCTAGAGATCCTGGACGATGAGGA ACACATCATCAGTTTCAGGGTTTTGGGAGGAGGCCACAGGTTGCAAAACTACTGGTCTGTTAC GTCCTTACACTCTCACGAGATTGATGGGCAGATGGGAACTCTAGTTCTGGAGTCTTATGTTGTAG ACATTCCTGAAGGTAACACCAGGGAGGAGACTCACATGTTTGTGGACACAGTTGTTCGTTGTA ACTTGAAAGCTTTGGCCCAGGTTTCAGAGCACAGATTTTTCCACGAGCTGAGAGCAAAAGAAC TATCCGCAGCGTCCTTGTCACTAGGCAGTAAAGAGGAAGCTGTGCATGCCAGGAAGAAGGAG GCTGTGCAAGTGTAG
PpPYL2	ATGATGCAGGAGAAACAGGGGCGGCCGGATTTCCAGTTCCTGTTGGAAGGGCAGCAGGATCT GATATGCCGGTTCCACAAGCACGAGTTGCTTCCGCACCAGTGCGGCTCCATCTTGTTGCAGCAG ATCAAGGCGCCTGTGCAGACCGTGTGGTTGATTGTGAGGAGGTTTGACGAGCCGCAGGTGTAC AAGCGGTTCATTCAGAGGTGTGACATCGTTGAAGGCGATGGCGTAGTGGGGAGCATCCGGGA GGTGCAATTAGTTTCTAGCATTCCCGCCACATCTAGCATCGAGAGGCTGGAAATTCTGGACGAT GAGGAGCATATCATCAGCTTCAGGGTCTTGGGAGGAGGCCATAGGTTGCAAAATTATTGGTCTG TGACTTCTTTGCACAGACATGAGATTCAAGGGCAGATGGGAACTCTAGTGCTGGAGTCTTATGT TGTGGATATTCCAGATGGTAACACAAGAGAGGAGACGCATACATTTGTGGACACAGTCGTGAG ATGCAATTTGAAAGCACTTGCTCAAGTCTCTGAGCAGAAACATTTGCTGAACTCCAACGAGAAA CCAGCGGCACCGTAG
PpPYL3 (Del 1-267)	ATGATGCAGCAAGTAAAGGGGCGGCAGGATTTCCAGAGGCTGCTGGAGGCGCAGCAGGATCT AATATGTCGTTACCATACTCACGAGCTGAAGGCTCACCAGTGCGGGAGCATCCTGCTGCAACAG ATTAAGGTGCCGTTGCCGATCGTGTGGGCGATTGTGCGCAGTTTCGACAAGCCTCAGGTCTACA AACGTTTTATTCAAACTTGCAAGATCACTGAAGGCGATGGTGGCGTGGGAAGCATCCGGGAGG TCCATCTGGTCTCCAGTGTTCCAGCCACTTGCAGTATTGAACGCCTCGAGATTTTGGATGATGAG AAACATATCATTAGCTTTCGGGTGCTGGGCGGGGGCCACCGTTTGCAGAACTACTCTTCCGTGT CATCTCTGCACGAGCTCGAAGTTGAAGGCCACCCTTGCACTCTCGTCCTGGAGTCGTATATGGTA GATATTCCCGATGGAAACACTCGCGAGGAGACGCATATGTTTGTGGATACTGTGGTTCGCTGCA ATTTGAAATCTTTGGCTCAGATTTCGGAGCAGCAGTATAACAAGGATTGTTTGCAACAGAAACA GCATGACCAGCAGCAGATGTATCAGCAGAGACACCCGCCACTTCCTCCTATTCCCATTACCGATA AAAATATGGAAAGGTCCAGTACTGTAATTTGCACCTGA
SmPYL1	CTGGTGCCGCGCGGCAGCCATATGAGCAGCAACGCATTGTCTAGGGAGGAGGAGCACATATGG CGCTACCACAAGCACGAGATGCAAGAGTATCAGTGTGGATCCATCCTCATCAAACGCATCAATG CGCCCGTGCAGCTGGTGTGGTCGCTCGTCCGGAGATTTGACCAACCGCAAGGCTACAAGAGAT TCATCCAGAGCTGCACTGTGAATGGCGATGGCAAAGTCGGGAGCATCCGAAACGTGAATGTGG TAACGGGGCTTCCAGCCACGAGCAGCACCGAGAGGCTGGAGATCCTGGACGAGGAGGAGCA CATCTTTAGTTACCGGATCCTTGGAGGAGATCATCGACTCAAGAATTACTGGTCTATAATCACGCT CCACTCCGAGATGATCAACGGTAGGCCCGGGACATTGGCGATCGAGTCGTACGTTGTGGACAC TCCCGAAGGGAACAGTAAGGAGGACACATGTTTCTTCGTGGAGACAGTGATCAAGTGCAACCT CAAATCATTGGCGGATGTGTCGGAGAGGCTTGCGCTGCAGACAAGCGTCGAGCACCTAACTTT GGCCTCCAGGAGTCCGTGACAAGCTTGCGGCCGCACTCG
SmPYL2 (Optimized)	CTGGTGCCGCGCGGCAGCCATATGGAAGAGGCAGTGGGTGAACACCACACACATGAGCCGGC CTCCAACGAGTGTTGTTCGGTTTTAGTACAGGAGGTACGTGCTCCTGTAGAGGTTGTCTGGTCA GTGGTACGGCGCTTCGACCAGCCACAGTGCTATAAGCGGTTCATACGGTCCTGCTCAACACAGG GAGATTTAAAGGTAGGCTCAACTCGCGAGATTACTGTTGTGTCGGGGCTTCCTGCAACTACGTC AAAAGAGCAGTTAGAGATCTTAGATGAGGATAAACACATACTTTCATTCAAAGTGTTGGACGGT GACCATCGTCTTCGGAATTACCGTAGCATCACTACTCTGCATGAGACTTTAGTCCAAGATCGCCC TGGTACACTGGTCATGGAGTCCTATGTCGTCGAGATCCCTGACGGGAACACCCGCGAGGACAC TCTTACTTTTACTAATACTGTGGTCAGATGTAACCTTCAATCGTTGGCGCGTACTTGTGAAAGACT TTTGCCCCACGCGGTTTAGCAAGCTTGCGGCCGCACTCG

SmPYL3 (Optimized)	CTGGTGCCGCGCGGCAGCCATATGTACCAACTTACTGACGAAGAGGTCGAGAAGTTGCCAGAA GAGGTTTGGGAATATCATAGAGCTCGTTCGGGCGGTGCCGGGATTGGCCCTAACGAATGCTGC TCTGTACTGATTCAACGTGTGCGTGCGCCTTTACCGGTTGTCTGGTCAGTCGTTCGTCGCTTCGA CAAGCCGCAGCTGTATAAGAATTTTATACGCTCCTGCTCATTTAAAGGTGACGAATTAAGAGTGG GATGTACGCGCGAAGTAACCGTAGTATCTGGACTGCCAGCCACGAGTAGTACGGAGAGATTAG AGATATTAGACGATGACAAACATGTGCTTTCCTTCCGTGTAGTTGGAGGGGACCACCGTCTTAAT AATTATCGCTCCGTAACATCACTGCACGAGTTCGATGTAGAAGGAGCGAAAGGTACGTTAGTGG TCGAGTCTTACGTGGTAGATGTACCGCCCGGAAACACAAGACAGGATACATGTCTTTTTACAGA TACCGTAGTTCGTTGCAATCTGCAATCCCTGGCACACATGACTGAAAAATTAGCGGTGGCCTGT GCTTCTGAACAACATCGCCAGCTTCACCAGGCCAGATGACAAGCTTGCGGCCGCACTCG
SmPYL4 (Optimized)	CTGGTGCCGCGCGGCAGCCATATGCTGGTCTCTTTAGGCGCTCTTGTACCGGATCAGGACGAG GCCGCCCGGTTGGTCGCGGCTGCGTCACGTTACCATTGCCATGCCCTTCGCGGCCACACGCAGT GTTCGAATGTTGTACCACAGTGGATACAGGCACCTGTTGCTGTAGTTTGGTCTGTTGTACGTCG GTTTGATTCTCCCCAAGCCTATAAGTGCTTCATCCGTGGTTGCGTGTTGCGGGAGGGGGATGGA GTATCCGTAGGCAGCACTCGGGACGTTACGTTGGTGAGTGGATTGCCCGCTAGTTGCAGCACC GAACGGCTTGAGATATTAGACGATCAACAGCATGTATTGTCATTCCGCGTCGTAGGAGGAGAAC ACAGACTTAAGAACTACACTTCGGTCACATCGCTGCACGCGACAACCGCCGGCGGCAGAGACG CGACGATAGTCCTTGAATCATATGTGGTAGATGTGCCGGCGGGGAACAGCAAAGAAGAAACCT TGACTTTTACTGATACGGTTGTTCGTTGTAATCTTCAGAGCCTGGCAAAAGTATGCGAACACTTA GCCCTTCAACAACAACAACAGCATCAGGATCGGTGACAAGCTTGCGGCCGCACTCG
SmPYL5 (Optimized)	CTGGTGCCGCGCGGCAGCCATATGTTAACGCCCCAACAGCGTTTACAATTAGACGAATCGCGTT GGCGCTTACACAGTGCTTTGAGCGCGGCACAACCGCACCAGTGTGCAAACTTACTGCTTCAGA GAATAGACGCACCCGTATCTGCCGTTTGGCCTATGTTGCGGCGTTTTGACACGCCCCAGGCATA CAAGAGATTCGTGAAGGCATGCGTCATCGCTTCTGGAGACGGCTCCAGTGTCGGGAGTCTTCG GAATATCACTCTGATCTCTGGATTGCCTGCATCATGTTCGACCGAGCGCTTAGAGATTTTGGATG ACGAGCATCATATAGTCTCCTTTCGTGTTGTCGGCGGCGAGCATCGTTTACGCAACTACGCTTCG GTCACGTCATTGCATGAGAAAGTGGTAACAGTAGTTATGGAGTCATACGTCGTCGATGTCCCTG AAGGAAACACTCGTGAAGATACGCGGGTTTTTACTGACACGGTGGTCAGATGTAACCTGCAATC TTTAGCGAAAATCTGCCAAGCGAACTTTAGACAGGAGCAACGTCGGTGTCAGCAACAACAGCA GCAGCAACCAGAGTGACAAGCTTGCGGCCGCACTCG
SmABI1	ATGGCTGTTTCGGGCACTGCTTGCAACAGGAGCACCCGCTGCATCGCCAGCGATACGTGTCCCC CGCATGGAGCCGTATTCATATGTGGCAGGCGCCGGGAGATGGAGGATGCCGTCGCGGTAGTGC CCTCTTTTATGACGGTGCCGTGCGGTACTGTTGGAGGCTGCGAGTGTAAAGGTGCCACGCTGC CTTCCGCGGACGTTGGCATGTCCGCGTTACACTTCTTCGGAGTCTATGACGGCCATGGCGGACC TCAGGTTGCTGGCTTCTGCAAGGAGCAAATGCATCGCGTCCTCGAGGAAGAGTTTAGTGGCGT TTTGCCAGGCATGGGTGACAGAGAGCTGGAGGCACATCTTCAGAGAGCAATGGTGGCGAGCT TTCTGAAAGTGGATGCGCAGGTGGGAGGCTTCCTCGAGGGCAATTTGAGTCCGTCAGCTTCTC CATTCATAGCTCCCGAGACAGTCGGCTCGACTGCTGTGGTAGCCGTACTGGGACCAAACCGGAT CATCGTCGCCAACTGTGGTGACTCGAGGGCCGTCCTTTCGAGAGGGGGGCGAGCCATTCCTCT CTCCGTGGACCACAAACCAGATCGAGAGGACGAGCTGGCCCGAGTTGAGGCTGCCGGAGGG AGGGTGTTTTTTTGGAACGGTTATAGAGTCTTAGGAGTTCTGGCAATGTCGAGAGCAATTGGT GATAGATACCTCAAGCCGTTTATAATCCCAGAGCCGGACGTTACTTGTACAGAGAGAAGTTCGG AGGACGAGTGCCTGATATTGGCCAGCGACGGCCTGTGGGACGTGCTCACCAACGAGATGGCG TGTGACATTGCACGGAAGTGTCTCGTTAGGCATCGAGCTCGGCAGGGCGGCGAGAGTGCCGC AGACATGGCTGCTGGATTACTGACCAAGGTCGCGATTGCCAAAGGCAGCACTGACAACATCAG TGTGGTGGTGGTGGATCTAAGCTCATCCATGCGAAGGTGA

SI Appendix, Table 3. List of accession number of all genes analyzed in this work.

Gene	Accession number
ZcPYL8	GFYA01000355.1
ZcABI1	GFYA01001477.1
MpPYL1	Mapoly0030s0080.1
MpABI1	GQ504039.1
PpPYL1	Pp3c26_15240V3.1
PpPYL2	Pp3c13_7110V3.1
PpPYL3	Pp3c7_26290V3.1
PpABI1A	Pp3c11_18330V3.1
SmPYL1	XM_002982810
SmPYL2	XM_002968967
SmPYL3	XM_002974543
SmPYL4	XM_002992701
SmPYL5	XM_024686983
SmABI1	XM_002980941
PYR1	AT4G17870
PYL1	AT5G46790
PYL2	AT2G26040
PYL3	AT1G73000
PYL4	AT2G38310
PYL5	AT5G05440
PYL6	AT2G40330
PYL8	AT5G53160
PYL9	AT1G01360
PYL10	AT4G27920
PYL11	AT5G45860
HAB1	AT1G72770
ABI1	AT4G26080
PEX4	AT5G25760